Editors' choice

Postcranial osteology of the first early-stage juvenile skeleton of *Plateosaurus trossingensis* from the Norian of Frick, Switzerland

DARIUS NAU, JENS N. LALLENSACK, URSINA BACHMANN, and P. MARTIN SANDER

Nau, D., Lallensack, J.N., Bachmann, U., and Sander, P.M. 2020. Postcranial osteology of the first early-stage juvenile skeleton of *Plateosaurus trossingensis* from the Norian of Frick, Switzerland. Acta *Palaeontologica Polonica* 65 (X): xxx–xxx.

Owing to monospecific mass-accumulation sites in Central Europe, the early-branching sauropodomorph *Plateosaurus* has one of the best fossil records among dinosaurs. Despite this, early-stage juveniles have been conspicuously absent. However, such specimens are critical in assessing the ontogenetic development of this taxon, as well as the role of heterochrony in sauropodomorph evolution. A new skeleton from the *Plateosaurus* bonebed at the Gruhalde Quarry (Klettgau Formation, Norian) of Frick, Switzerland, nicknamed "Fabian", represents the first substantially complete juvenile referrable to *Plateosaurus*. The specimen includes large portions of the cranium and vertebral column and an almost completely represented appendicular skeleton. Its juvenile ontogenetic stage is confirmed by a lack of neurocentral suture fusion in the axial skeleton. Consistent with this, the estimated total length and body mass of approximately of 2.3 m and 40 kg are considerably smaller than any previously reported specimen of the genus. Surprisingly, the postcranial morphology of the specimen is remarkably consistent with that of osteologically mature individuals, including a virtually fully developed pattern of laminae and fossae in the vertebrae. Comparisons of body proportions are complicated by varying degrees of compaction in the limb elements, but skeletal proportions mostly appear to follow isometry, with the notable exceptions of a relatively long neck, proportionately larger manus, shorter, more gracile humerus and shorter forearm in the juvenile specimen. The observed morphology suggests that adult morphology was either achieved early in ontogeny of *Plateosaurus*, or alternatively that developmental plasticity, which has previously been found to result in high variability of adult body size, could potentially also extend to morphological development.

Key words: Dinosauria, Sauropodomorpha, morphometrics, morphology, small body size, early ontogeny, Triassic, Swiss Plateau.

Darius Nau [dariusnau@uni-bonn.de], Section Paleontology, Institute of Geoscience, University of Bonn, Nussallee 8, 53115 Bonn, Germany.
Jens N. Lallensack [info@dinospuren.de], Section Paleontology, Institute of Geoscience, University of Bonn, Nussallee 8, 53115 Bonn, Germany; School of Natural Sciences and Psychology, Liverpool John Moores University, James Parsons Building, Bryon Street, Liverpool L3 3AF, UK.
Ursina Bachmann [urbach@gmx.ch], Sauriermuseum Frick, Schulstrasse 22, 5070 Frick, Switzerland.
P. Martin Sander [martin.sander@uni-bonn.de], Section Paleontology, Institute of Geoscience, University of Bonn, Nussallee 8, 53115 Bonn, Germany; Dinosaur Institute, Natural History Museum of Los Angeles County, 900 Exposition Boulevard, Los Angeles, CA 90007, USA.

Received 9 April 2020, accepted 15 July 2020, available online 3 November 2020.

Introduction

Plateosaurus from the Upper Triassic of Central Europe is among the best-represented dinosaur genera in the world, owing largely to its occurrence at three large, almost monospecific mass accumulations in Germany and Switzerland (von Huene 1907–1908; Fraas 1913; Jaekel 1914; Galton 1986; Sander 1992).

A multitude of species of *Plateosaurus* have been named (e.g., von Huene 1932), and uncertainty remains regarding the number and identity of valid species. Most *Plateosaurus* material, including that from Frick, Trossingen, and Halberstadt, is traditionally referred to a single species. Weishampel and Chapman (1990) conducted a morphometric study of *Plateoaurus*-femora from Trossingen and suggested the presence of two weakly distinguishable, potentially sexual

morphs of a single species at the locality, but did not draw a conclusion as to the identity of this species. It has usually been identified as either *Plateosaurus longiceps* (Galton 2000, 2001; Galton and Upchurch 2004), its possible senior synonym or nomen dubium *Plateosaurus erlenbergiensis* (Galton 2000; Prieto-Márquez and Norell 2011), or synonymized with the original type species *Plateosaurus engelhardti* which has been variously considered to include all or most *Plateosaurus* material (Galton 1984, 1985, 1986; Moser 2003; Yates 2003) or to be relatively uncommon and restricted in its distribution (Galton and Upchurch 2004). However, Galton and Kermack (2010) proposed a taxonomic separation between Trossingen and Halberstadt specimens, referring the former to *Plateosaurus trossingensis* and restricting the usage of *P. longiceps* to the latter. Yates (2003) did not distinguish *P. longiceps*, *P. trossingensis*, and *P. erlenbergiensis* from *P. engelhardti*, but erected a second species, *P. gracilis*, for some of the older material previously referred to *Sellosaurus*. *Gresslyosaurus ingens* from the Norian of Switzerland has been referred to *Plateosaurus* as *Plateosaurus ingens* (e.g., Yates et al. 2010) or considered a synonym of *P. engelhardti* (Galton 1986) or a nomen dubium (Galton 2001) but has recently been proposed as generically distinct from *Plateosaurus* pending a revision of the material (Rauhut et al. 2020). The diagnostic utility of the type material of *P. engelhardti* and its synonymity with the speces erected for more complete skeletons recovered in major localities such as Trossingen has been a matter of ongoing debate (see Galton 2001, 2012; Sues 2013). Most recently, following an application by Galton (2012) and comments by Sues (2013) and Galton (2013), *P. trossingensis* (Fraas 1913) has been declared as the new type species (ICZN 2019), based on a skeleton (SMNS 13200) first mentioned and named by Fraas (1913) and described in detail by von Huene (1926). We provisionally consider the other material from Frick and Trossingen to be referrable to this species.

Unequivocally juvenile material has thus far not been described for *Plateosaurus*, with the exception of some isolated vertebrae that exhibit open neurocentral sutures, but essentially adult body size (Hofmann and Sander 2014). This lack of juveniles can be explained by the presence of a taphonomic filter, miring in mud, which prevented the preservation of individuals below a certain body-mass threshold (Sander 1992). *Plateosaurus* individuals from Frick and Trossingen display no clear correlation between adult body size and age so that size alone is no reliable indicator of maturity, which, under the assumption that only one species is present in these samples, has been explained as a consequence of developmental plasticity (Sander and Klein 2005; Hofmann and Sander 2014).

Here we describe the postcranium of a new, juvenile skeleton of *Plateosaurus* cf. *trossingensis* (Sauriermuseum Frick, MSF 15.8B.) discovered at Frick, Switzerland (Fig. 1B). The specimen represents the first substantially complete find of a juvenile *Plateosaurus*, as well as the first such specimen with a body size significantly below the known adult size range of the taxon at approximately half the linear size of the smallest reported adults. As such, it provides previously unavailable evidence on the morphology during the early ontogeny of this taxon, and an opportunity to study features that are frequently linked to ontogeny, such as postcranial skeletal pneumaticity and limb proportions. The specimen represents an exceptional case of preservation of a small-bodied individual in a bonebed otherwise exclusively composed of large-bodied individuals.

Institutional abbreviations.—GPIT, Geologisch-Paläontologisches Institut und Museum, Tübingen, Germany; MSF, Sauriermuseum Frick, Frick, Switzerland; SMA, Sauriermuseum Aathal, Aathal-Seegräben, Switzerland; SMNS, Staatliches Museum für Naturkunde, Stuttgart, Germany.

Other abbreviations.—acdl, anterior centrodiapophyseal lamina; acpl, anterior centroparapophyseal lamina; c, cervical vertebrae (numbered from anterior, c1, atlas; c2, axis); ca, caudal vertebrae (numbered from anterior); cdf, centrodiapophyseal fossa; cpol, centropostzygapophyseal lamina; cprl, centroprezygapophyseal lamina; d, dorsal vertebrae (numbered from anterior); dc, distal carpal; mc, metacarpal (numbered I–V from preaxial/anterior side); MOS, morphological ontogenetic stages; mt, metatarsal (numbered I–V from preaxial/medial side); p, (non-ungual) phalanx; pacdf, parapocentrodiapophyseal fossa; pcdl, posterior centrodiapophyseal lamina; pcpl, posterior centroparapophyseal lamina; pocdf, postzygocentrodiapophyseal fossa; podl, postzygodiapophyseal lamina; ppdl, parapodiapophyseal lamina; prcdf, prezygocentrodiapophyseal fossa; prdl, prezygodiapophyseal lamina; prpadf, prezygoparapodiapophyseal fossa; prpl, prezygoparapophyseal lamina; prsl, prespinal lamina; spof, spinopostzygapophyseal fossa; spol, spinopostzygapophyseal lamina; sprf, spinoprezygapophyseal fossa; sprl, spinoprezygapophyseal lamina; tpol, intrapostzygapophyseal lamina; tprl, intraprezygapophyseal lamina; u, ungual.

Material and methods

Find MSF 15.8. consists of several individuals preserved in a roughly circular bone cluster, including a disarticulated juvenile skeleton, nicknamed “Fabian” and designated MSF 15.8B., found scattered near the tail of a larger skeleton (MSF 15.8A., see Fig. 1C). The specimen was discovered during the annual salvage excavation campaign in the Gruhalde Quarry of the Tonwerke Keller AG (Fig. 1A) supervised by Ben Pabst (MSF/SMA) in 2015. The skeleton was fully excavated in 2016 and is now housed at the municipal Sauriermuseum, Frick, Switzerland. With the exception of the left pes and some delicate ribs, the entire specimen has been fully prepared and is freed of adhering matrix.

The present work provides a full description of the postcranial morphology of this specimen. The cranial material

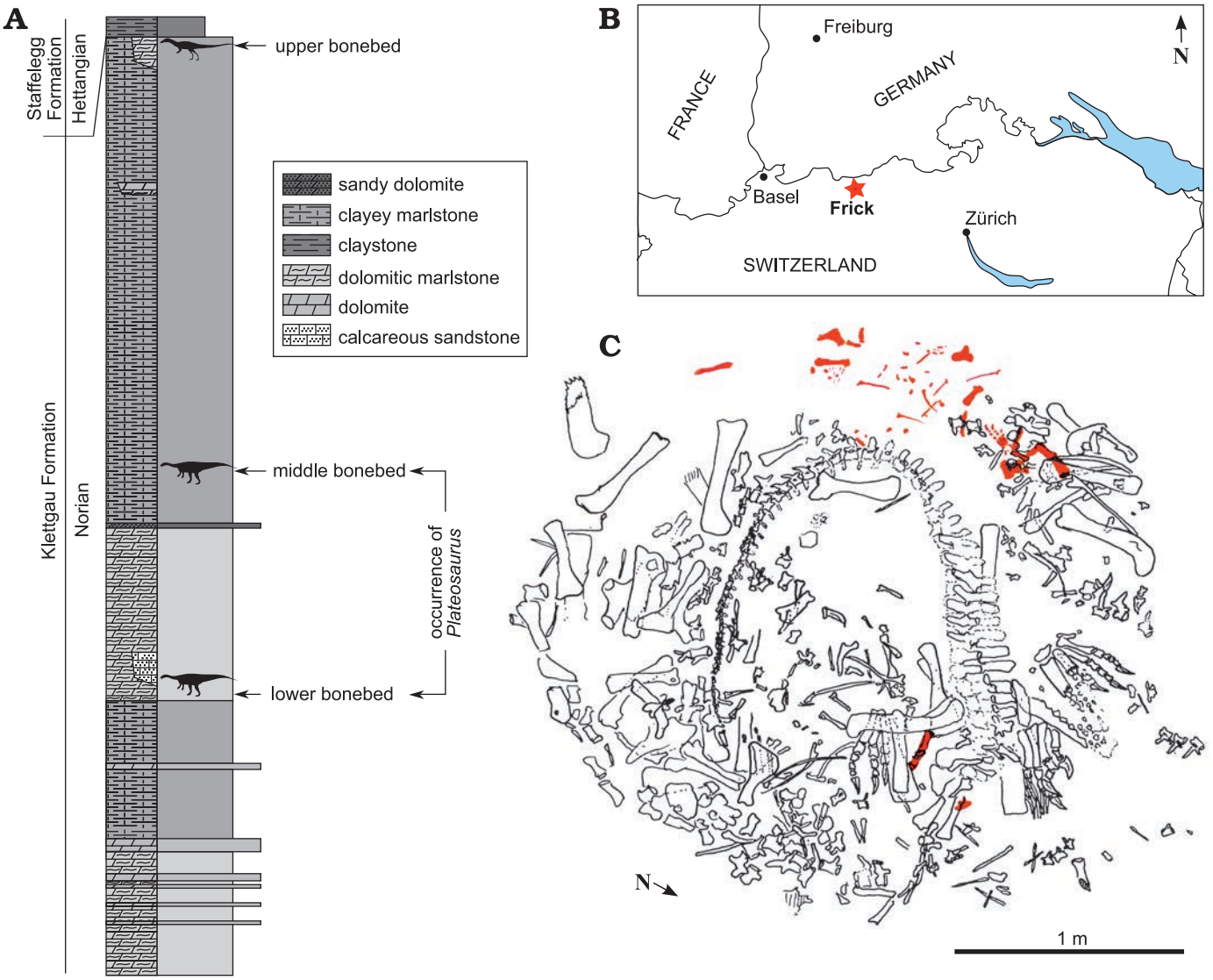

Fig. 1. **A**. Stratigraphic section of Gruhalde Member (Klettgau Formation) exposed at Gruhalde Quarry in Frick (redrawn from Jordan et al. 2016). **B**. Location of Frick in northern Switzerland (asterisk). **C**. Excavation map of bone concentration MSF 15.8., juvenile *Plateosaurus* cf. *trossingensis* skeleton MSF 15.8B. in red (after Ben Pabst, used with permission).

pertaining to the skeleton will be described together with adult cranial material of *Plateosaurus* from the same locality at a later date by one of us (JNL).

Due to its association with adult material, the identification of individual elements as pertaining to the juvenile skeleton was based on consistent size and, where applicable, the absence of suture closure. The material is of matching size and none of the elements are represented double. Due to this, the relative completeness of the skeleton, and the great rarity of juvenile and (especially) small-bodied *Plateosaurus* specimens, this being the first and only such find, we therefore consider assignment to a single individual to be more parsimonious than an accumulation of several small individuals without preserved overlapping material.

Unless specified, the anatomical nomenclature in the present work follows Romer (1976). Description of the vertebral laminae and fossae follows the nomenclature established by Wilson (1999) and Wilson et al. (2011), with some additions as outlined by Carballido and Sander (2014). Morphological ontogenetic stages (MOS) for vertebral elements, as defined by Carballido and Sander (2014), are applied to *Plateosaurus*, following Hofmann and Sander (2014). MOS 1–3 denote early, middle, and late immature individuals, with a progressively greater number of observable morphological features (mainly vertebral laminae and fossae) but retaining unfused neurocentral sutures, while MOS 4 and 5 are adults with closed neurocentral sutures, but different degrees of development of some neural arch features.

The material was subject to a high degree of post-mortem deformation as a result of sediment compaction during diagenesis, as evident from stark differences between the left and right sides of the skeleton. The axis along which the skeletal elements are compacted depends on their orientation during diagenesis, e.g., the humerus, which was embedded in the sediment vertically, is compacted along its long axis. Accordingly, in describing the morphological effects

of compaction, this axis of compaction will be described with respect to the anatomical orientation of the individual bones. The degree of compaction varies between individual specimens and bones, but is generally more pronounced in Frick material than in that from other *Plateosaurus* bonebeds, and appears to be especially strong in the material described here, possibly as a result of poor ossification compared to other individuals.

The anatomical standard for comparison of the juvenile material are the almost complete, articulated skeletons SMNS 13200 (Fraas 1913; von Huene 1926; holotype of *P. trossingensis*), GPIT 1 and 2 (von Huene 1928, 1932; Mallison 2010a, b; Reiss and Mallison 2014; DN personal observation) and MSF 23 (Sander 1992 and DN personal observation). Additionally, juvenile neural arches from Frick, described by Hofmann and Sander (2014), whose morphology is broadly consistent with adult morphology, were used for comparison.

Measurements up to 150 mm were taken to the nearest 0.1 mm using sliding callipers. Measurements greater than 150 mm were taken to the nearest mm using a ruler or tape measure. All measurements represent straight-line distances, unless specifically noted otherwise. Mass estimates were calculated using R (R Core Team 2018) and phylogenetically corrected cQE (mathematically corrected scaling equation for bipeds based on data from quadrupeds, R package "MASSTIMATE"; Campione 2016).

Photos were taken with a Canon® EOS 700D, an 18–135 mm zoom lens and 13–31 mm extension tubes. Scale bars refer to the flat surface of the object closest to the camera, and are less accurate for parts of the fossil that are further in the background.

Systematic palaeontology

Dinosauria Owen, 1841

Sauropodomorpha von Huene, 1932

Plateosauridae Marsh, 1895

Genus *Plateosaurus* von Meyer, 1837

Type species: *Plateosaurus trossingensis* Fraas, 1913 from the Knollenmergel (Trossingen Formation) of Trossingen, Baden-Württemberg, Germany, Norian, Upper Triassic (ICZN 2019)

Plateosaurus cf. *trossingensis* Fraas, 1913

Material.—MSF 15.8. was recovered from the Middle Saurian Level ("Mittlere Knochenschicht" or "Mittlere Saurierbank"), Gruhalde Member, Klettgau Formation at Gruhalde Quarry, Frick, Switzerland (Norian; Jordan et al. 2016). MSF 15.8B. (nicknamed "Fabian") nearly complete, disarticulated skeleton of a juvenile individual. The material includes a large part of the skull (premaxilla, dentary, prefrontal, squamosal, parietal, basisphenoid and parasphenoid, all to be described in a separate paper), the atlas, axial neural arch and four complete postaxial cervical vertebrae, six dorsal vertebrae, one isolated probable anterior dorsal centrum and three isolated dorsal neural arches. The sacrum is represented by a single isolated neural arch and the tail by three isolated proximal and mid-caudal neural arches, four isolated mid-caudal centra, a complete distal caudal vertebra and five haemal arches. Three cervical and 12 dorsal ribs, parts of the gastral basket and a single disarticulated caudal rib are preserved. The limb girdles are almost complete, with only the clavicles and left pubis missing. The limb skeleton is also essentially completely represented, but is missing some phalanges of the manus and pes, and ulna, tibia, fibula, and parts of the manus and pes are only preserved on one side.

Description.—*Axial skeleton*: The osteology of the axial skeleton is broadly consistent with that of adult *Plateosaurus trossingensis* individuals. All neurocentral sutures are open, resulting in dissociation of centra and neural arches, with the notable exception of a single distal caudal. Since most vertebrae have been subjected to varying degrees and angles of compaction, isolated centra do not always represent a good fit for their respective neural arches, and their positional assignment should be treated as tentative. Due to this deformation, which distorts the centrum height and width measurements, morphometrics are of limited use in characterising original centrum shapes (SOM: table S1 in Supplementary Online Material available at http://app.pan.pl/SOM/app65-Nau_etal_SOM.pdf). The ratio between centrum length and the mean of centrum widths and heights is herein used as an approximate indicator of centrum shape (hereafter referred to as an "elongation index").

The precaudal vertebral count in *Plateosaurus* is 10 cervical vertebrae, 15 dorsal vertebrae, and 3 sacral vertebrae (von Huene 1926), the last of which is a caudosacral (Yates 2003). There are a minimum of 45 caudal vertebrae (Mallison 2010b).

Morphological complexity in the cervical series of *Plateosaurus* increases posteriorly (due to the superpositional expression of hox genes; Böhmer et al. 2015), as is also observable in MSF 15.8B. Cervical vertebrae (Fig. 2) are long and relatively low, with proportionately low neural spines that gradually decrease in anteroposterior length and increase in height in more posterior vertebrae. In anterior cervicals, both costal articulations are located near the anterior margin of the centrum, but the diapophysis migrates onto the neural arch in the mid-cervical region (sensu Böhmer et al. 2015). In posterior cervicals, diapophyses increase in size, resulting in the width measured across these processes slightly exceeding the length measured between the zygapophyses. The centra are elongated in the anterior and mid-cervical region, with elongation indices in the range of 2.8–3.5, but are shorter in the posterior cervicals (index of 2.0 in c9). Based on the average length of centra and neural arches, the neck of the juvenile skeleton is estimated to be slightly longer in proportion to the dorsal vertebrae than in adult individuals (SOM: table S6).

Dorsal vertebrae (Figs. 3 and 4) are anterioposteriorly short and dorsoventrally tall compared to the cervicals, and their centra are wider, less elongated (elongation indices of

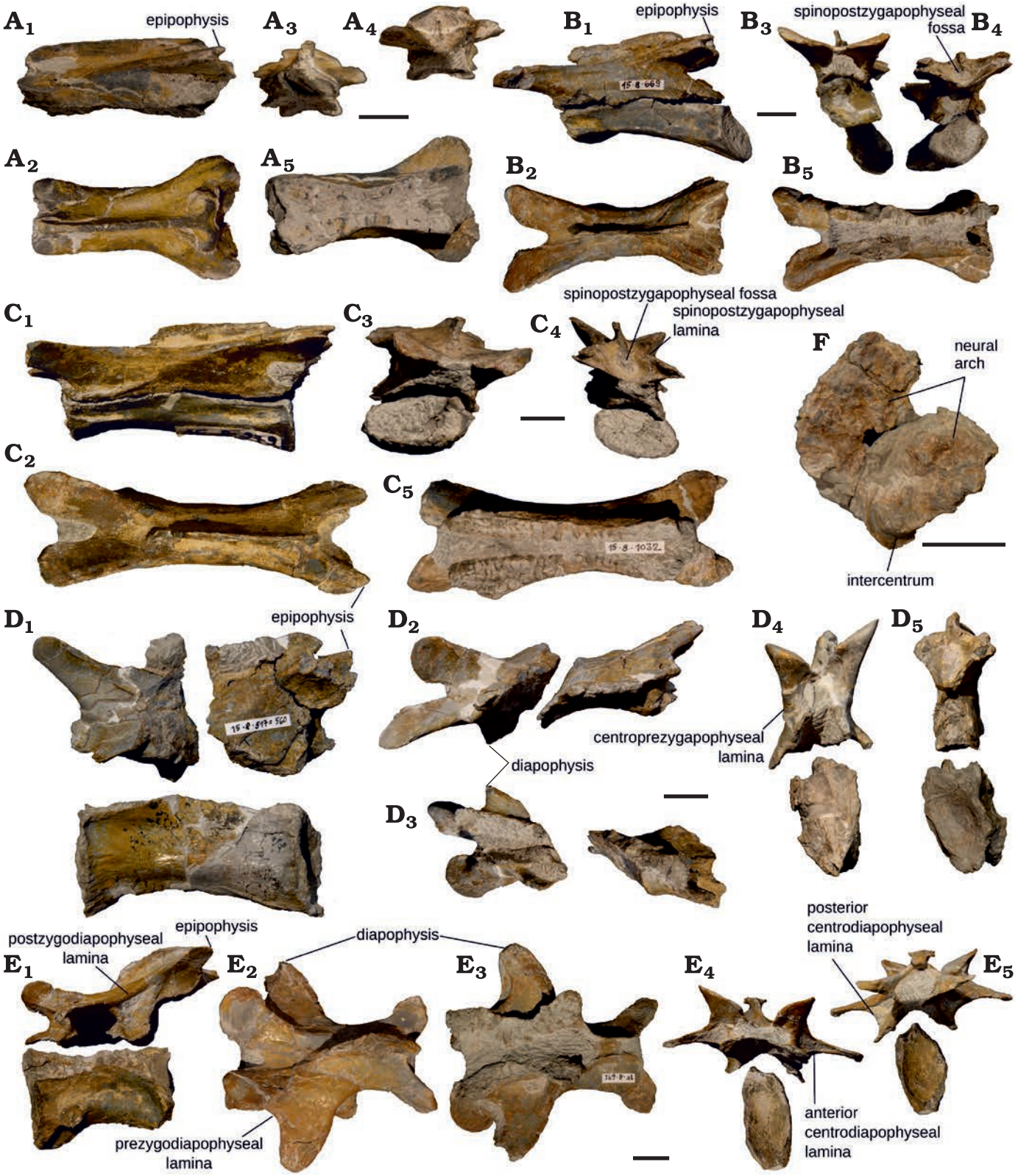

Fig. 2. Cervical vertebrae of juvenile *Plateosaurus* cf. *trossingensis* Fraas, 1913 skeleton MSF 15.8B. from the Norian of Frick, Switzerland. **A**. Cervical vertebra 2 (axis), MSF 15.8.2001, in left lateral (A_1), dorsal (A_2), anterior (A_3), posterior (A_4), and ventral (A_5) views. **B**. Cervical vertebra 3, MSF 15.8.669 (neural arch) and MSF 15.8.936 (centrum), in left lateral (B_1), dorsal (B_2), anterior (B_3), posterior (B_4), and ventral (B_5) views, **C**. Cervical vertebra 4, MSF 15.8.1032 (neural arch) and MSF 15.8.979 (centrum), in left lateral (C_1), dorsal (C_2), anterior (C_3), posterior (C_4), and ventral (C_5) views. **D**. Cervical vertebra 6, MSF 15.8.2002 (neural arch) and MSF 15.8.592 (centrum), in left lateral (D_1), dorsal (D_2), ventral (D_3), anterior (D_4), and posterior (D_5) views. **E**. Cervical vertebra 9, MSF 15.8.671 (neural arch) and MSF 15.8.905 (centrum), in left lateral (E_1), dorsal (E_2), ventral (E_3), anterior (E_4), and posterior (E_5) views. **F**. Cervical vertebra 1 (atlas), MSF 15.8.2000, in ?anterior view. Centra are omitted in ventral view to show neural arch. Scale bars 10 mm.

1.1–1.7) and more strongly constricted along their middle. Hyposphenes are present, where this region is well preserved, but hypantra are often obscured by matrix and an articulation in the fossil material cannot be achieved. Overall morphology and lamination pattern of the vertebrae are identical to previously described material of *Plateosaurus* (e.g., von Huene 1926; Hofmann and Sander 2014). Posterior cervicals and anterior dorsals of some *Plateosaurus* specimens, including SMNS 13200, show an incipient dorsal bifurcation of the neural spine (von Huene 1926), but others (e.g., GPIT 1, Mallison 2010a and MSF 23, DN personal observation) do not. Bifurcation was not observed in any of these neural spines in MSF 15.8B., but it is unclear whether this is a preservational artefact and/or could be related to the state of ossification. On all precaudal vertebrae, the neurocentral sutures are open and arches and the centra are completely dissociated.

Where they are sufficiently preserved, the ventral, unfused suture surfaces of all neural arches are sculptured with a characteristic "zipper-like" pattern (sensu Hofmann and Sander 2014).

Detailed descriptions of the individual vertebrae are provided below.

Atlas: The preserved parts of the atlas (MSF 15.8.2000, Fig. 2F) are a small, wedge-like bone interpreted as the intercentrum and a partial neural arch consisting of two halves, exposed on matrix from the anterior or posterior side. The preserved portions of the neural arch are broad and wing-like, and an acute posterior process is not preserved.

Axis, neural arch: The axial neural arch (MSF 15.8.2001, Fig. 2A) is elongated (48 mm long anteroposteriorly and 14 mm tall dorsoventrally). No matching centrum was recovered, hence the diapophysis and parapophysis are not preserved. The neural spine is very long anteroposteriorly (35 mm) and low dorsoventrally (6 mm), with its flat dorsal margin gently sloping downwards anteriorly. The neural spine is relatively uniform in transverse width (ca. 2 mm) throughout its length, except for a slight expansion to ca. 3 mm anteriorly. Its posterior end bifurcates into two prongs that then curve around anterolaterally and terminate above the epipophysis at roughly half the distance between the midline and lateral edge of the vertebra. Instead of connecting to the postzygapophysis (to form a spol), this structure forms a deep vertical rim above the epipophyses.

The prezygapophyseal facets are set on incipient processes near the anterior end, elevated ca. 5 mm above the base of the pedicles. They face slightly dorsolaterally for articulation with the atlas. The postzygapophyses are more distinct and span a wider distance than the prezygapophyses. The epipophyses are thin, lightly striated sheets of bone and slightly overhang the postzygapophyses posteriorly.

Because the small space between the prezygapophyses is obscured by matrix, the presence of a tprl and sprl can not be ascertained. Cprl, cpol, and tpol are present.

The pedicles are strongly constricted transversely in the middle of the vertebra in an hourglass-like shape and diverge towards the ends; with their anterior expansion being wider than the posterior one.

Cervical vertebra 3, neural arch and centrum: c3 consists of a neural arch (MSF 15.8.669, Fig. 2B) and a centrum (MSF 15.8.936) found to fit with the former. It is identified as c3 based on its smaller size as opposed to the otherwise similar succeeding vertebrae (von Huene 1926).

The neural arch is proportionately taller than that of the axis and larger overall (57 mm long and 18 mm tall). The neural spine is slightly shorter anteroposteriorly (31 mm) and approximately the same dorsoventral height as in the axis (6 mm), and its dorsal margin is more rounded and thickens posteriorly. At both ends, it slightly overhangs its base, a probable artifact of deformation.

The prezygapophyses are much longer than those on the axis, extending out beyond the neural spine and pedicles at a low angle for ca. 10 mm and separated by a deep medial notch. The articular facets are mostly aligned dorsally and very slightly medially. The postzygapophyses are shorter but span roughly the same width, with the articular surfaces mostly facing downwards. Small, knob-shaped epipophyses are present.

Tprl, cprl as well as tpol and cpol are present. An incipient sprl is present, but very weakly developed. The same applies to the sprf. By comparison, the spol and spof are more pronounced.

The pedicles are taller than in the axis, and centrally constricted, albeit less markedly than in the axis. Once again, the transverse expansion is more pronounced anteriorly.

The centrum (maximum height 14 mm) is amphicoelous, with the concavity on the anterior surface being much shallower than on the posterior surface, and has been subjected to strong posterodorsal compaction. This has resulted in the ventral surface being displaced posteriorly so that the anterior articular surface faces anteroventrally and the posterior one posterodorsally. The diapophysis and parapophysis are located at its anterodorsal and anteroventral margin respectively. Both of these articulations have accessory posterior laminae, which are separated by an elongated fossa. The ventral surface of the centrum is mostly flat, with a weakly developed medial ridge being visible in the posterior third. The centrum has an elongation index of 3.1.

Cervical vertebra 4, neural arch and centrum: The neural arch (MSF 15.8.1032, Fig. 2C) referred to c4 is ca. 1/3 longer than c, but as a result of the dorsoventrally low (5 mm) neural spine and probably some dorsoventral compaction, the arch height as preserved is marginally lower (17 mm).

The anterior and posterior margins of the anteroposteriorly long (36 mm) neural spine are incompletely preserved, giving them a sloped appearance. The transverse width of the arch is comparable to the previously described c3. The prezygapophyses are longer than the postzygapophyses and separated by a deep notch. The postzygapophyses are overhung dorsally by short, pointed epipophyses. Both prezygapophyseal and postzygapophyseal articular surfaces are close to horizontal. Tprl, cprl, tpol, and cprl are present,

as are a well-developed spol and spof. Sprl and sprf are also present, but still quite weakly developed, albeit slightly more pronounced than in c3. No other fossae apart from sprf and spof are present on this neural arch.

The pedicles are tall, as in the previous vertebrae. The sculptured ventral suture surface is especially well-preserved in this vertebra. In ventral view, the pedicles are constricted centrally and widest anteriorly, but due to the greater elongation of the vertebra, this change in width occurs less abruptly than in the previous vertebrae.

The dorsoventrally compressed centrum (MSF 15.8.979) is amphicoelous, but the anterior concavity is mostly hidden by matrix. The small, knob-like costal articulations are located at its anterior end, separated by a shallow horizontal fossa. The diapophysis is located at the neurocentral suture, from where a weak ridge extends onto the neural arch, running posterodorsally towards the postzygapophysis without reaching it. The parapophysis is located closer to the ventral rim of the centrum. The ventral surface is flat and delimited laterally by ridges extending posteriorly from the diapophyses in the anterior third of the centrum. The elongation index of the centrum is 3.5.

Cervical vertebra 6, neural arch and centrum: The neural arch (MSF 15.8.2002, Fig. 2D) of this vertebra is preserved as two fragments, the anterior one of which consists of the prezygapophyses, the diapophyses and the anteriormost portion of the neural spine, while the posterior fragment encompasses the postzygapophyses and most of the neural spine. The neural arch (31 mm) and spine (13 mm) are relatively tall compared to the preceding vertebrae, and the presence of a diapophysis on the arch supports its more posterior position. The arch bears signs of strong transverse compaction, with an additional shearing component in the sagittal plane, as shown by the different orientations of the diapophyses. The neural spine is similar in anteroposterior length, but much taller than in preceding vertebrae.

The zygapophyseal facets are set at an almost vertical angle, which is at least in part a result of compaction. The prezygapophyses are large and rounded and are supported ventrally by thick cprl and medially by a weak tprl. There are well-developed sprl enclosing a shallow sprf. The postzygapophyses are incompletely preserved, with parts of their posterior edges missing, but they appear to have been relatively short but overhung by pointy epipophyses. There is a well-developed spol and spof. The cpol are narrower than their anterior equivalents, but still well developed.

The diapophyses are two small, subtriangular processes that extend ventrolaterally from the anterior portion of the ventral edge of the neural arch, overhanging the centrum. There is a weak lamina connecting the diapophysis anteriorly to the base of the prezygapophysis. Incipient laminae extend anteroventrally from the postzygapophysis and posterodorsally from the diapophysis, constituting the beginnings of a podl, but the two do not form a well-defined connection. No well-developed fossae are present apart from the spinoprezygapophyseal fossa in this arch. The tall pedicles are only weakly constricted centrally, bear sculptured suture-surfaces and diverge slightly further anteriorly.

A transversely compacted centrum (MSF 15.8.592) missing part of its anterior surface is a possible fit for the neural arch based on its size, elongation and the presence of a single, long median ventral keel, which support its assignment to the 6th cervical position, but the diagenetic deformation of both arch and centrum makes a definite assignment difficult. A shallow depression runs across the lateral surface for much of the length of this centrum. No parapophysis is preserved, which is interpreted as a result of the poor preservation of the rims of this centrum. The centrum elongation index is 2.8.

Cervical vertebra 9, neural arch and centrum: The neural arch of c9 (MSF 15.8.671, Fig. 2E) differs significantly from the preceding vertebrae in its proportions and the well-developed diapophyses, whose width even surpasses the zygapophyseal length. This identifies it as a posterior cervical by comparison with adult individuals, among which it is most similar to c9 based on relative size and neural arch morphology (e.g., von Huene 1926).

The neural spine is shifted posteriorly, overhanging the pedicles and centrum. It is relatively short anteroposteriorly (31 mm), and its dorsal margin is rounded and sloped anteriorly. The top of the spine bears a transverse expansion of ca. 8 mm, probably as a result of compaction.

The prezygapophyses are shorter and more rounded, and their facets face more medially than those in the more anterior vertebrae. Tprl, cprl, and sprl are present, along with a very shallow sprf. The postzgapophyses overhang the posterior margin of the pedicles and centrum and are themselves overhung posteriorly by prominent epipophyses, which form the posteriormost points of the vertebra. Such elongate epipophyses are present in *Plateosaurus* individuals from Trossingen (*P. trossingensis*, SMNS 13200, von Huene 1926; included under *P. engelhardti*, sensu Yates 2003), but are not found in specimens from Halberstadt (Jaekel 1914; Yates 2003; *P. longiceps*, sensu Galton and Kermack 2010). Spol and cpol are well-developed, whereas the tpol is very thin. There is a deep spof.

The diapophysis forms a prominent process extending laterally and in a slight anterior curve from the center of the neural arch. The width of the vertebra measured across the diapophyses is slightly greater than its zygapophyseal length. The diapophyses are supported by all the usual diapophyseal laminae, which are well-defined in this vertebra (acdl, pcdl, cprl, cpol) and the fossae delimited by these laminae (prcdf, cdf, pocdf) are also well-developed.

The pedicles are comparatively short both anteroposteriorly and dorsoventrally compared to the rest of the arch. They diverge anteriorly and posteriorly, the anterior expansion being the more marked one of the two.

MSF 15.8.905 is an isolated, transversely crushed centrum. Its prominent parapophysis is located further dorsally and posteriorly than in preceding vertebrae. It has a well-developed acpl, running towards the ventral edge of the

centrum, and a shorter, less defined pcpl. The assignment of this centrum to this vertebra is tentative, because the extreme transverse compaction precludes a good fit with the pedicles of the neural arch. At an elongation index of 2.0, this centrum is much shorter than the more anterior cervicals, in accordance with its position close to the cervicodorsal transition.

?Dorsal vertebra 1, centrum: This centrum (MSF 15.8. 2003, Fig. 3A) is here tentatively assigned to the first dorsal position based on the presence of a large, subtriangular parapophyseal facet at the neurocentral juncture and a (poorly preserved) medial ventral keel. The centrum has been subjected to slightly oblique, mostly transverse shearing deformation, resulting in extensive distortion of the orientation of its amphicoelous articular surfaces. Compared to preceding centra, it is very short and deep. The centrum is strongly constricted along the middle. The elongation index is 1.3.

Dorsal vertebra 2, neural arch and centrum: Neural arch (MSF 15.8.908, Fig. 3B) is dorsoventrally tall (32 mm), anteroposteriorly short (45 mm), and very wide (63 mm). The proportions of the arch, shape of the neural spine and lack of any trace of a parapophysis on the arch suggest an anterior position within the dorsal column, and its postzygapophyses fit well with the prezygapophyses of the (presumed) succeeding vertebra, suggesting the arch pertains to d2. The neural arch has been subjected to deformation with a primary axis from posterodorsal to anteroventral, resulting in the neural spine and zygapophyses being displaced anteriorly relative to the pedicles.

The slightly anteriorly inclined neural spine (probably at least in part due to the aforementioned compaction) of this vertebra is one of the anteroposteriorly shortest (13 mm) and transversely thickest (9 mm) in the entire vertebral column, with a width of ca. 70% of the anteroposterior length.

The prezygapophyses are elongate processes with rounded ends and subhorizontal facets. The postzygapophyses are shorter and more vertical, with the articular facets facing ventrolaterally. Both cprl and cpol are strongly developed, with the latter split into medial and lateral divisions. The sprl are very short and weak and a sprf appears to be absent or so inconspicuous as to be hidden by matrix. The spol are particularly prominent and enclose a deep spof. The tprl is deeply recessed and only visible from the ventral side. There are no distinct epipophyses in this vertebra.

The diapophyses have large, ovoid articular facets set on broad, winglike processes, joined to the zygapophyses and to the pedicles by prominent prdl and podl, acdl and pcdl. The prdl is almost straight, whereas the podl is more deeply curved. The prcdf, cdf, and pocdf are also well-developed. The posterior end of the pedicles is pushed so far posteriorly due to deformation that in dorsal view, the pcdl is visible behind the more concave margin of the podl.

The pedicles are thick but lack the central constriction present in cervical neural arches.

The neural arch offers a potential fit for an isolated, amphicoelous centrum (MSF 15.8.978). The centrum is transversely compressed, rendering a definite assignment to d2 difficult, but it bears a large parapophyseal facet at the neurocentral suture, ca. 1/3 of its length from the anterior end, and a prominent ventral medial keel. The dorsal portion of the lateral face bears a shallow fossa running along the length of the centrum. The centrum elongation index is 1.7.

Dorsal vertebra 3, neural arch and centrum: Neural arch (MSF 15.8.2004, Fig. 3C) is dorsoventrally tall (46 mm), anteroposteriorly short (42 mm), and transversely wide (67 mm). Based on these proportions, the morphology of the neural spine and the lamination pattern observed, this vertebra pertains to the anterior dorsal region. The extreme anteroposterior shortness of the neural spine is especially characteristic of the second, third, and fourth dorsal, with d3 bearing the anteroposteriorly shortest neural spine in SMNS 13200 (Jaekel 1914; von Huene 1926). A parapophysis is not discernible on the neural arch; it would have been located mostly or entirely on the centrum (von Huene 1926), which was not found for this vertebra. This suggests a more anterior position relative to the otherwise very similar arch MSF 15.8.477, and the fit between the zygapophyses of these vertebrae support this assignment.

The neural spine of this vertebra is the shortest anteroposteriorly in the entire presacral collumn (12 mm) but is thick transversely (ca. 8 mm). The neural spine is moderately tall when measured from its base (21 mm) but protrudes only a short distance above the high-set postzygapophyses.

The prezygapophyses are missing parts of their anterior margin, but are relatively shorter and more rounded than in the preceding vertebrae, which is consistent with the situation in the anterior dorsals of adults. There is a strong cprl, whereas the tprl is weak and receding, bordering a shallow sprf. A weakly defined sprl is present. The prezygapophyseal articular surface faces dorsomedially, but are more horizontal than vertical. The postzygapophyseal surfaces point in a more lateral than ventral direction. The base of the tpol is connected to a (postero)medial division of the cpol, whereas a lateral division continues dorsally to the dorsal tip of the postzygapophysis, with the articular surface (and a shallow fossa) bordered by these laminae. This feature is reminiscent of the condition described in cervical vertebrae of *Europasaurus* (Carballido and Sander 2013), but comparatively only weakly developed, and is also present in a previously described *Plateosaurus* d3 from Frick (see Hofmann and Sander 2014: fig. 7C).

The diapophyses are large, wing-like processes originating near the middle of the vertebra, slightly closer to the anterior end, and sloping slightly posteriorly and downwards (the latter probably being a diagenetic feature). The width across the diapophyses is ca. 60% greater than the maximum length (= zygapophyseal length sensu Hofmann and Sander 2014) of the neural arch. There are strong anterior and posterior centrodiapophyseal laminae and ventral diapophyseal fossae (prcdf, cdf, pocdf) as well as well-developed prdl and podl,

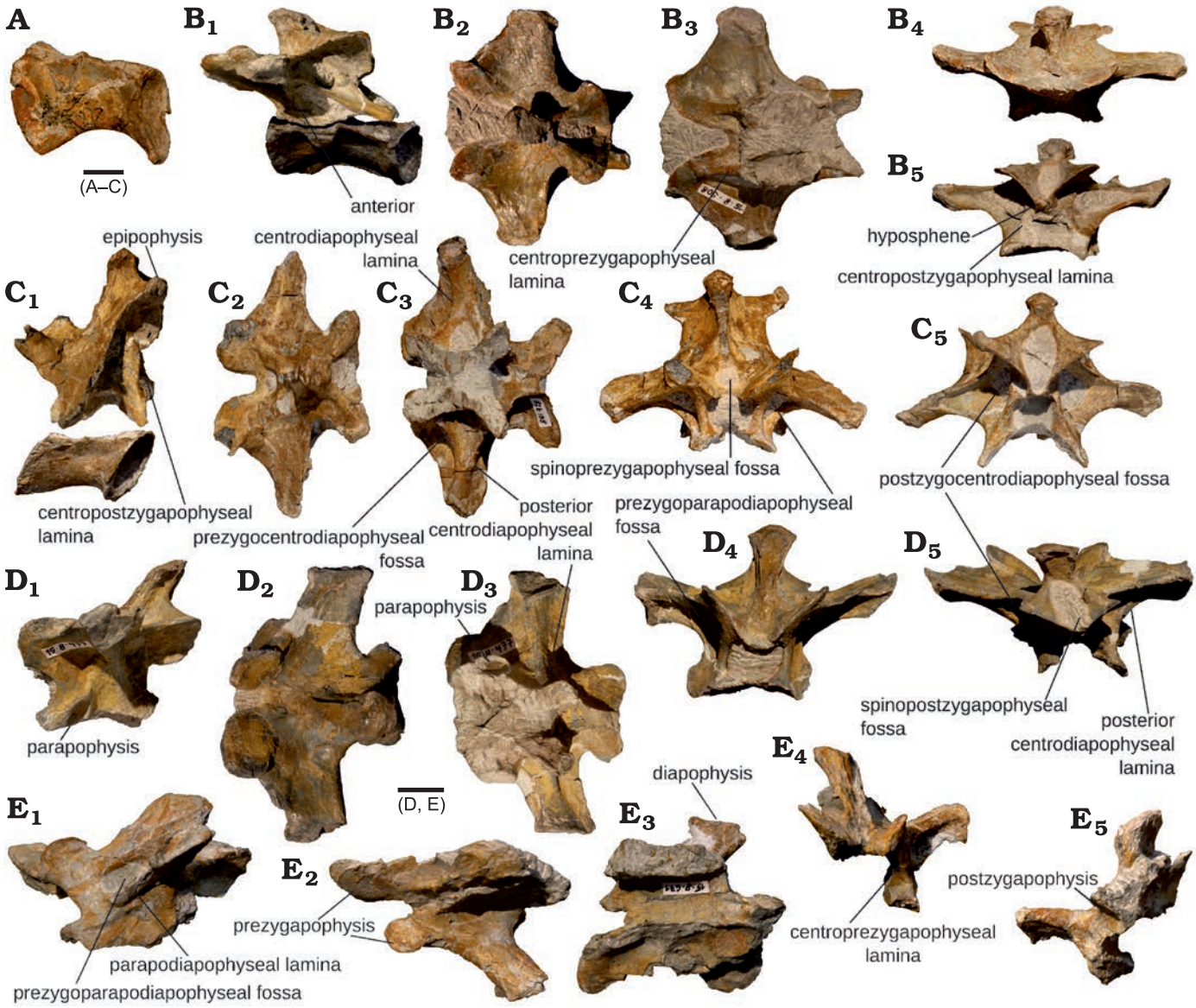

Fig. 3. Anterior dorsal vertebrae of juvenile *Plateosaurus* cf. *trossingensis* Fraas, 1913 skeleton MSF 15.8B. from the Norian of Frick, Switzerland. **A**. Centrum of ?dorsal vertebra 1, MSF 15.8.2003, in left lateral view. **B**. Dorsal vertebra 2, MSF 15.8.908 (neural arch) and MSF 15.8.978 (centrum), in left lateral (B_1), dorsal (B_2), ventral (B_3), anterior (B_4), and posterior (B_5) views. **C**. Dorsal vertebra 3, MSF 15.8.2004 (neural arch) and MSF 15.8.2005 (centrum), in left lateral (C_1), dorsal (C_2), ventral (C_3), anterior (C_4), and posterior (C_5) views. **D**. Dorsal vertebra 4, MSF 15.8.477, in left lateral (D_1), dorsal (D_2), ventral (D_3), anterior (D_4), and posterior (D_5) views. **E**. Dorsal vertebra 5, MSF 15.8.2006, in left lateral (E_1), dorsal (E_2), ventral (E_3), anterior (E_4), and posterior (E_5) views. Centra are only depicted in lateral view. Scale bars 10 mm.

bordering a weak sprf. The diapophyses have been subjected to some deformation causing them to be depressed ventrally.

The pedicles of this neural arch are centrally constricted, the posterior margins diverge further than the anterior ones.

The centrum (MSF 15.8.2005) is slightly wider than tall, strongly constricted centrally and compacted from anterodorsal to posteroventral, so that its articular faces are oblique rather than vertical. Roughly 1/4 of its length behind the anterior margin of its right side, a small, subtriangular parapophyseal facet is preserved at the neurocentral suture, confirming the identity of MSF 15.8.2005 as an anterior dorsal centrum. This facet is not preserved on the left side. There is a shallow depression covering most of the dorsal half of the centrum in lateral aspect. The anterior and posterior parts of the ventral and lateral surfaces of the centrum bear strong striations. The elongation index is 1.2.

d4, neural arch: This isolated neural arch (MSF 15.8.477, Fig. 3D) is slightly shorter than the aforementioned two, but it is identified as a d4 by the presence of partial parapophyseal facets at the neurocentral sutures, suggesting a more posterior position. In other *Plateosaurus* individuals, the parapophysis is located entirely on the centrum in d1 and d2, and migrates partially onto the neural arch in d3 to d5, until it is located entirely on the arch by d6 (von Huene 1926). Since roughly half of the facet seems to be present on the arch, this is consistent with assignment of the arch to d4.

The arch as a whole appears to be relatively unaffected by deformation, with only the prezygapophyses bearing obvious traces of some compaction.

The neural spine is short and thick, but is slightly longer and more teardrop-shaped in dorsal aspect as opposed to squarish. The prezygapophyses are very short and wide and protrude only weakly from the prdl. They have a distinctly rounded shape, being the culmination of a trend towards this shape in the anterior dorsals. This development appears to be somewhat more pronounced than in adults. There is a weak sprl and sprf. The postzygapophyses, joined medioventrally by a tpol, are overhanging the posterior end of the pedicles. The postzygapophyses are set at a slightly more horizontal angle than the very steep prezygapophyses. Spol and spof are well developed and both prezygapophyses and postzygapophyses are connected to the pedicles by pronounced cprl and cpol. The epipophysis is indistinct from the dorsal margin of the postzygapophysis, and remains so in the rest of the dorsal series.

The diapophyseal facet is large and roughly triangular as seen in lateral aspect. The processes are somewhat narrower (anteroposteriorly) than in the preceding vertebrae and directed slightly posteriorly. The prdl, podl, ppdl, and pcdl are all well developed and delimit deep prpadf, pacdf, and pocdf. The parapophysis is situated at the ventral end of the anterior diapophyseal lamina, which is consequently a ppdl in this arch, and is bisected by the neurocentral suture. Since the facet extends down to the neurocentral suture, there is no cpl. The preserved part of the articular facet appears to have an ovoid shape when completed with the part located on the (missing) centrum. The pedicles of this vertebra are very tall and centrally constricted.

?Dorsal vertebra 5, fragmentary neural arch: This fragment of a dorsal neural arch (MSF 15.8.2006, Fig. 3E) consists of both prezygapophyses, the neural spine, left diapophysis and fragmentary left postzygapophysis, left pedicle and neural canal. Based on the shape of the neural spine, closely resembling d4, and the somewhat more elongated prezygapophyses, an assignment to the position of d5 is tentatively suggested.

The neural spine is thick and teardrop-shaped in dorsal view, but narrower and longer than in the preceding vertebrae.

Both pairs of zygapophyses seem to have been set at a fairly steep angle in this arch. The prezygapophyses are rounded and large, but more elongated than in the preceding vertebra. They are supported by well-developed cprl and sprl and a tprl, enclosing a sprf. The postzygapophyses likewise are connected to a well-developed spol, but tpol, cpol and spof are not preserved.

The diapophysis is a long, straight and relatively narrow process with a distal expansion and a relatively large articular facet, in continuation of a trend observable in the preceding few vertebrae. The poorly preserved parapophysis, which is bordered dorsally by the end of the ppdl, is an elongated, ovoid facet extending from close to the front of the pedicles diagonally to roughly the middle of the arch. There are strong prdl and podl, a deep but narrow prpadf, and a shallower and smaller pacdf. The pcdl is subvertical in lateral aspect. A pocdf may have been present, but is broken off along with the posterior end of the pedicles.

Dorsal vertebra 6, neural arch and centrum: The neural arch (MSF 15.8.654, Fig. 4A) is identified as a 6th dorsal by its greater length (50 mm) and the combination of its tall, long neural spine and anteroposteriorly long zygapophyses with a discontinuous prdl and the presence of a well-developed prpl. The arch has been subjected to some deformation, resulting in the neural spine being bent to the left and slightly anteriorly.

The neural spine of this vertebra is much narrower (3 mm) and anteroposteriorly longer (32 mm) than in the anterior dorsals. Its anterior margin is concave, so that the anterior corner of the apex overhangs the base.

The prezygapophyses are elongated and narrow, the postzygapophyses small. Due to the location of the parapophyses near the anterior margin of the pedicles, there is a thick prpl in place of a cprl, whereas the cpol are relatively thin and deeply recessed from the posterior margin of the postzygapophyses. The tprl is only visible ventrally, and the sprfa is either obscured by matrix, or absent. A small spof is present. The zygapophyses are set at a relatively flat angle, possibly as a result of compaction.

The diapophyses are flat processes that take the shape of rounded trapezoids in dorsal view, with a crescent-shaped articulation facet (with a convex ventral margin). They are joined to the zygapophyses by a relatively well developed prdl and podl. The diapophysis is connected to the oval parapophysis by a relatively short and weak ppdl and to the posterior part of the pedicles by a much thicker pcdl. There are well-developed infra-diapophyseal fossae (prpadf, pacdf, and pocdf). The parapophyseal facet is round and located at the neurocentral suture. There is a lateral bulge formed by the laminae above the parapophysis as seen in dorsal aspect.

The pedicles are almost straight in ventral view, with very little transverse expansion being present towards the ends.

The transversely compacted, amphicoelous centrum (MSF 15.8.906) bears a shallow concavity along the dorsal half of its lateral surface, whereas the bottom of the centrum is rounded. Near both ends, the ventral and lateral faces bear light striations. The elongation index of the centrum is 1.6.

Dorsal vertebra 7, neural arch and centrum: The neural arch (MSF 15.8.1076, Fig. 4B) of this vertebra is similar in shape to the preceding d6, but is longer (57 mm) and differs in its shorter prezygapophyses and complete loss of the prdl.

The neural spine is anteroposteriorly long (41 mm) and very arrow (2 mm), bearing some evidence of anterodorsal compaction (resulting in a crushed anterodorsal margin). The prezygapophyses are relatively short, pointed and slightly curved. The prezygapophyses are connected directly to the parapophyses, which in this vertebrae occupy the anteroventral corner of the neural arch, by a ventrolaterally directed prpl. Sprl and sprf are present. The postzygapophyses overhang the pedicles, and are supported by

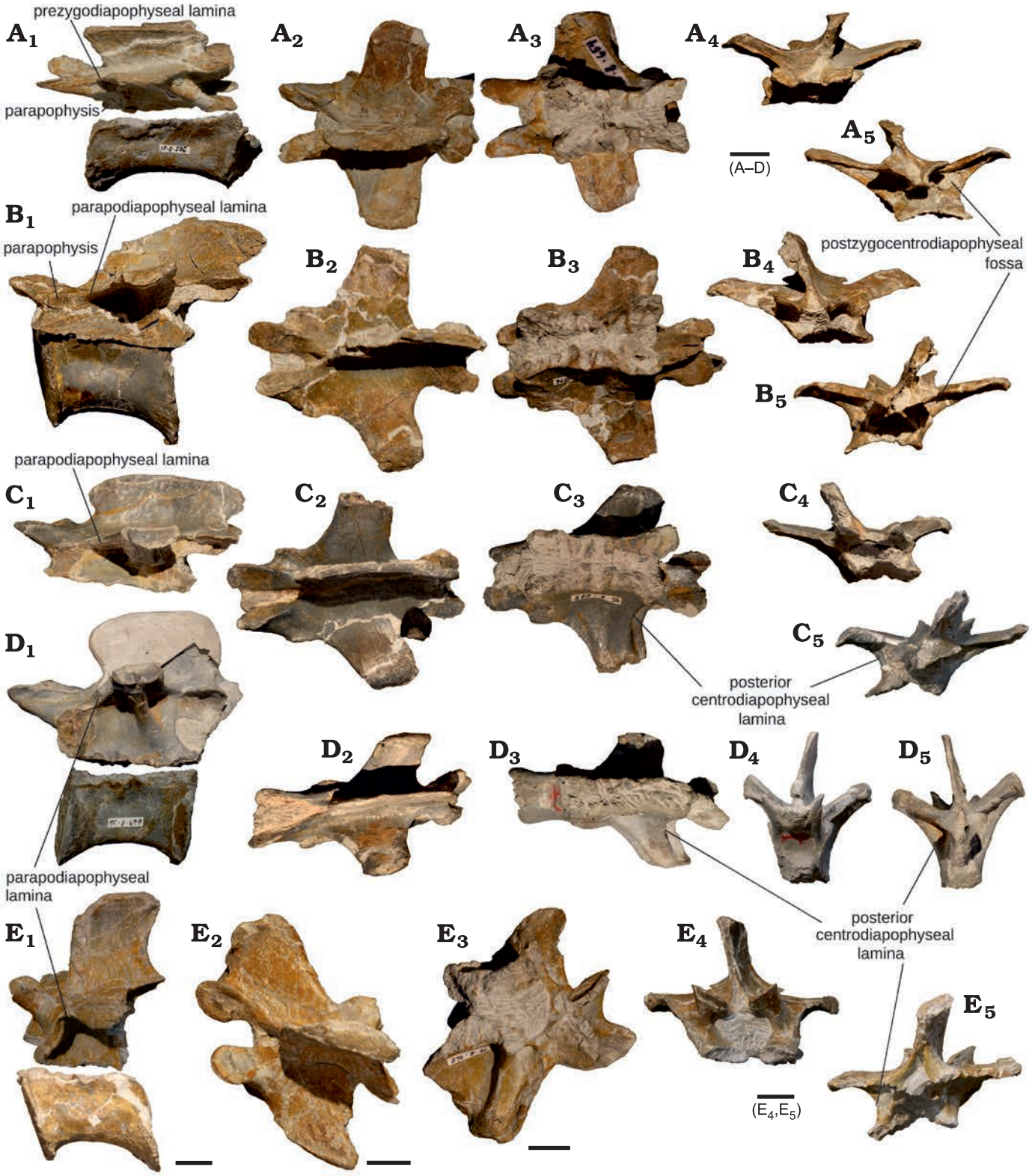

Fig. 4. Middle and posterior dorsal vertebrae of juvenile *Plateosaurus* cf. *trossingensis* Fraas, 1913 skeleton MSF 15.8B. from the Norian of Frick, Switzerland. **A**. Dorsal vertebra 6, MSF 15.8.654 (neural arch) and MSF 15.8.906 (centrum), in left lateral (A_1), dorsal (A_2), ventral (A_3), anterior (A_4), and posterior (A_5) views. **B**. Dorsal vertebra 7, MSF 15.8.1076 (neural arch) and MSF 15.8.437 (centrum), in left lateral (B_1), dorsal (B_2), ventral (B_3), anterior (B_4), and posterior (B_5) views. **C**. Dorsal vertebra 8, MSF 15.8.885, in left lateral (C_1), dorsal (C_2), ventral (C_3), anterior (C_4), and posterior (C_5) views. **D**. Dorsal vertebrae 9 or 10, MSF 15.8.728 (neural arch) and MSF 15.8.679 (centrum), in left lateral (D_1), dorsal (D_2), ventral (D_3), anterior (D_4), and posterior (D_5) views. **E**. Dorsal vertebra 12, MSF 15.8.468 (neural arch) and MSF 15.8.2007 (centrum), in left lateral (E_1), dorsal (E_2), ventral (E_3), anterior (E_4), and posterior (E_5) views. Scale bars 10 mm.

a strongly curved cpol and a weak spol, enclosing a small spof. The zygapophyseal pairs are each angled at slightly less than a right angle.

The diapophyses are trapezoid in dorsal view, with their posterior edges forming an angle close to 90° with the sagittal plane. They bear anteroposteriorly long and dorsoventrally flat articular faces. The pcdl and podl are well-developed. In this vertebra, the ppdl and prpl replace the prdl, with the parapophysis being expanded dorsally and anteriorly to interrupt this lamina. A pronounced lateral bulge is present in the dorsal outline above the parapophyses. There are only two diapophyseal fossae, the pocdf and pacdf. The pedicles are relatively narrow and sub-parallel, with a slightly wider posterior expansion.

The centrum (MSF 15.8.437) that is tentatively assigned to this vertebra based on its good fit with the neural arch is amphicoelous and bears some traces of anterodorsal compaction. Its ventral surface is convex, and lightly striated towards the margins, whereas the dorsal part of the lateral surface bears an anteroposterior depression. The elongation index of this centrum is 1.4.

Dorsal vertebra 8, neural arch: This neural arch (MSF 15.8.885, Fig. 4C) strongly resembles the preceding one in terms of length (58 mm) and proportions, but has shorter and more posteriorly directed diapophyses and a larger parapophyseal facet.

Its neural spine is anteroposteriorly long (41 mm) and narrow (2 mm), spanning the entire medial length of the vertebra, with its dorsal margin being almost uniformly tall throughout its length. Both its anterior and its posterior margins are concave, so that the dorsal corners are overhanging their base.

The prezygapophyses are thin and pointed, with elongate articular facets. As in the preceding vertebrae, a prpl takes the place of the cprl. Weak sprl are present, but there is no discernable sprf. The postzygapophyses overhang the base of the neural arch. Cpol and very thin spol and tpol, which enclose a small spof, are present.

The diapophyses are more posteriorly oriented and shorter than in the preceding vertebrae. They are dorsoventrally flat, bearing elongate, kidney-shaped facets. The podl is relatively short and concave, and a thin pcdl is present, connecting it to the posterior end of the neurocentral suture. The parapophysis is located in the anterior corner of vertebra, braced posterodorsally against the diapophysis by a ppdl and antrodorsally against the prezygapophysis.

The ppdl is almost horizontal, because the parapophysis still links the diapophysis and prezygapophysis, forming ppdl and prpl. The fossae present ventral to the diapophysis are the pocdf and pacdf. The pedicles are broad and relatively straight.

Dorsal vertebra 9/dorsal vertebra 10, neural arch and centrum: The neural arch (MSF 15.8.728, Fig. 4D) of this vertebra is long (57 mm), tall (40 mm) but extremely narrow (35 mm) as a result of transverse compaction. The tall (21 mm), narrow (2 mm) neural spine and more posteriorly deflected diapophyses than in the preceding vertebrae suggest d9 or d10 as the position of this arch, but the transverse compaction precludes a good articulation with the preceding vertebrae.

The dorsal portion of the neural spine is broken off, but the fragment fits the rest of the spine. The neural spine is narrow, somewhat shorter anteroposteriorly (32 mm) than in preceding vertebrae and concave anteriorly.

The prezygapophyses are large, with their relatively broad surfaces set at an unnaturally steep angle by the transverse deformation. Sprl, and prpl are present. The postzygapophyses overhang the centrum, as in previous vertebrae, but the cpol is comparatively straight. Spol and a small, narrow spof are present.

The diapophysis is trapezoidal in shape and swept posteriorly. It is thicker than in the preceding vertebrae, although this condition might be amplified by the deformation. The diapophyseal articular surfaces are large and roughly semicircular in shape. The anterior edge is interrupted dorsal to the large parapophyseal facet and does not reach the prezygapophysis to form a prdl. The diapophysis is braced ventrally by a pcdl and posteriorly by a weakly developed dpol. Almost parallel to the anterior margin, a narrow ppdl extends anteroventrally, bracing the diapophysis against the parapophysis. Again, only pocdf and pacdf are present ventral to the diapophysis. The pedicles are very tall, narrow as a result of compaction, and almost completely parallel.

A long, amphicoelous centrum (MSF 15.8.679) is tentatively assigned to this vertebrae based on its size and apparent fit with the neural arch. There is a shallow, lateral concavity on the dorsal half of the centrum, and the ventral and lateral surface are weakly striated towards the articular margins. The centrum elongation index is 1.5.

Dorsal vertebra 12, neural arch and centrum: The neural arch (MSF 15.8.468, Fig. 4E) is shorter (42 mm) and more massive overall than in the preceding vertebrae, bearing a taller, transversely thickened and anteroposteriorly shorter neural spine. The differences in proportions and the tall (22 mm), thick (7 mm) and anteroposteriorly short (23 mm) neural spine suggests a position around two or three vertebrae more posterior than d9. There is some minor deformation from the right posterolateral direction as evident from the deformation of the transverse processes.

The prezygapophyses are short, rounded processes extending strongly anterodorsally. The zygapophyseal facets are set at a relatively horizontal angle. Sprl, tprl and a small sprf are present. The prezygapophyses are braced against the ventral end of the parapophysis by a prpl. The overhanging postzygapophyses are incomplete ventrally. Spol, spof, and cpol, pcdl and pacdf and a small pocdf are present.

The diapophysis is rounded in dorsal view and dorsoventrally thick, and it appears to extend out straight laterally if compaction is ignored. The parapophyseal facet is elongated in dorsoventral direction and connected to the diapophysis by a ppdl. There is a short but very thick acpl. The pedicles

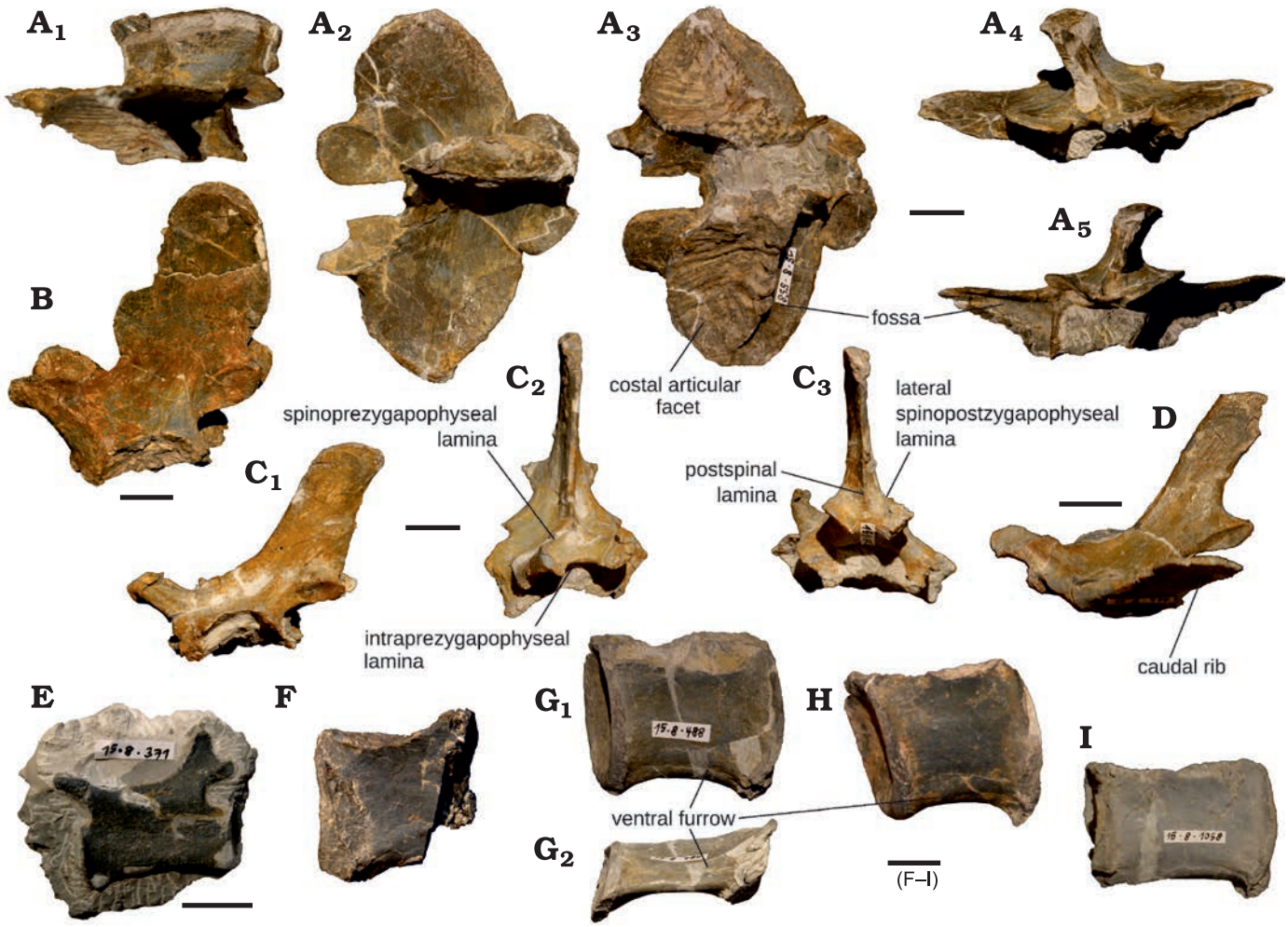

Fig. 5. Sacral and caudal vertebrae of juvenile *Plateosaurus* cf. *trossingensis* Fraas, 1913 skeleton MSF 15.8B. from the Norian of Frick, Switzerland. **A**. Sacral neural arch, MSF 15.8.558, in left lateral (A_1), dorsal (A_2), ventral (A_3), anterior (A_4), and posterior (A_5) views. **B**. Anterior caudal neural arch, MSF 15.8.889, in left lateral view. **C**. Mid-caudal neural arch, MSF 15.8.972, in left lateral (C_1), anterior (C_2), and posterior (C_3) views. **D**. Mid-caudal neural arch, MSF 15.8.476, in left lateral view (note fused transverse process). **E**. Distal caudal vertebra, MSF 15.8.371 (note closed neurocentral suture), in left lateral view. **F**. Proximal caudal centrum, MSF 15.8.2008, in lateral view. **G**. Proximal caudal centrum, MSF 15.8.488, in lateral (G_1) and ventral (G_2) views. **H**. Proximal caudal centrum, MSF 15.8.975, in lateral view. **I**. Mid-caudal centrum, MSF 15.8.1058, in lateral view. Scale bars 10 mm.

are wider and shorter than in preceding vertebrae, and expanded posteriorly.

Like the arch, the amphicoelous centrum (MSF 15.8.2007) is very broad and robust. Its transverse width is greater than its dorsoventral height, and it is strongly constricted. The ventral surface is convex and striated near the margin. The dorsal part of its lateral surface bears a well-developed, anteroposteriorly elongate fossa. This is the proportionately shortest presacral centrum preserved, at an elongation index of 1.1. This is the most posterior dorsal vertebra represented in the skeleton.

Sacral vertebra, neural arch: This isolated neural arch (MSF. 15.8.558, Fig. 5A) is interpreted as a first sacral based on its rectangular neural spine and wide transverse processes that extend relatively straight laterally, each bearing a single, large and heavily sculptured articular surface for the (missing) sacral ribs anteroventrally. The neural arch is flattened dorsoventrally (28 mm) and moderately long anterioposteriorly (49 mm), with its transverse width of 69 mm being its largest dimension by a considerable margin. The neural spine is long anteroposteriorly (32 mm) and relatively thick transversely (8 mm), with a straight, horizontal dorsal margin.

The prezygapophyses are large, teardrop-shaped facets emanating from the rounded anterior margins of the transverse processes. A sprl and sprf are absent, but the zygapophyses are braced ventrally against the costal articulation by a thick prdl or prpl. The postzygapophyses are rounded in dorsoventral view, with a strongly convex dorsal margin that joins the posterior margin of the transverse processes. The postzygapophyses are joined medially by a well-developed tpol and braced ventrally by a thin cpol. Both pairs of zygapophyses are set at relatively horizontal angles.

The anteroposteriorly broad, rounded transverse processes are ovoid in dorsal view and lightly striated mediolaterally. The lightly concave suture surface for the attachment of the sacral rib covers approximately the anteroventral 2/3

of each transverse process, being delimited posteriorly by the pcdl (applying the homology suggested by Wilson 1999). There are narrow, transversely elongated pocdfs situated behind these laminae.

The pedicles are relatively broad and short, each pedicle being subtriangular in shape as seen in ventral view, with their widest portions in the middle of the arch and thinning out towards the anterior and posterior ends.

Proximal caudal neural arch: This tall, laterally compressed neural arch (MSF 15.8.889, Fig. 5B) is interpreted as a proximal caudal due to lack of fused transverse processes (caudal ribs) and the tall (36 mm) and anteroposteriorly long (30 mm) neural spine, the latter characterizing anterior caudal vertebrae of *P. engelhardti* (sensu Yates 2003, including *P. trossingensis*). The spine has a rounded apex and bears a rounded protrusion on its anterior margin. The caudal ribs were unfused and are not preserved. Their articular surfaces are large, semicircular concavities on the sides of the neural arch, extending down to the neurocentral suture. In ventral aspect, these facets appear as deep concavities in the lateral margins of the pedicles.

The prezygapophyses are rounded processes extending anterodorsally from the neural arch and are supported ventrally by robust cprl. A prominent tprl and sprl and a small sprf are present. The postzygapophyses are located high on the neural arch, protruding slightly from the concave posterior edge of the neural spine, to which they are connected by spol, enclosing a small spof. Ventrally they are connected to the base of the neural arch by strong cpol. The zygapophyses are very narrow, and their facets are set almost vertically. The pedicles are very broad and shallow.

Middle caudal neural arch 1: Like MSF 15.8.889, this neural arch (MSF 15.8.972, Fig. 5C) lacks the transverse processes. It resembles the only slightly larger MSF 15.8.889 in being proportionately tall and narrow, with a tall neural spine, but differs with respect to the shape and anteroposterior length of the neural spine and the shape of the zygapophyses and facets for the transverse processes.

The neural spine is dorsoventrally lower (27 mm), anteroposteriorly shorter (15 mm) and more angular than in the preceding example, and is more sloped backwards. The suture surfaces for the transverse processes present as anteroposteriorly elongate, dorsoventrally narrow depressions in the lateral surface of the base of the arch, with a pronounced, laterally overhanging dorsal rim. The prezygapophyses are parallel rimmed in lateral view, but rounded in ventral view, extending straight out anterodorsally. Again, tprl, sprl, and sprf are present. The small, pointed postzygapophyses are placed further dorsally, protruding behind the posterior margin of the neural spine and beyond the posterior end of the pedicles. While the cpol are very strongly developed, the tpol and spof are absent. Unlike in the preceding vertebrae, where the spol emanates from the posterior margin of the neural spine (medial spol), this vertebrae bears lateral spinopostzygapophyseal laminae and a postspinal lamina instead. This region of the neural spine is frequently poorly preserved and only rarely figured, precluding comparisons with most specimens, but a postspinal lamina is also figured (though not mentioned) in some caudal vertebrae of *P. engelhardti* from Bavaria described by Moser (2003).

The pedicles are shallow and very broad anteriorly, becoming narrower posteriorly where they adjoin the articular facet for the transverse process.

Middle caudal neural arch 2: Unlike in the preceding vertebrae, here the transverse processes are fully fused to the arch (MSF 15.8.476, Fig. 5D). The assignment of this arch to "Fabian" is nonetheless supported, on the basis of its small size and overall proportions, which suggest a more posterior position than specimen MSF 15.8.972. The arch is ca. 80–90% the size of MSF 15.8.972 in all dimensions except for the neural spine, which is slightly taller dorsoventrally (32 mm), but shorter anterioposteriorly (12 mm), making it a more gracile. The prezygapophyses are small and more horizontal than in the preceding vertebra, with their facets set at ca. 45° to the horizontal. There is a well-developed prsl, branching into the two sprl at its ventral end, and a tprl. The postzygapophyses are overhanging the pedicles at the posteroventral edge of the neural spine, as in the preceding vertebrae; their facets are subvertical and connected to weakly developed spol and strong cpol. The transverse processes are long and flat, anteroposteriorly long as compared to the neural spine and, slightly tapering from their base to their subrectangular ends.

Isolated caudal centra: The four preserved isolated caudal centra (Fig. 5F–I) are assignable to the proximal or mid-caudal region based on their size and proportions. An exact positional assignment is not feasible based on the limited features available. In SMNS 13200, the first six caudal centra as tall as or taller than long, with length/height-ratios between 0.75 and 1.0 (von Huene 1926), which is not the case in any of the complete caudal centra recovered for "Fabian", but some centra approach the upper bound length/height-ratio of 1.0, suggesting they could have been positioned in or just slightly behind this region of the tail when accounting for individual and ontogenetic variation.

The centra are characterised by rounded antero- and posteroventral corners, forming the attachment points of the haemal arches. All preserved caudal centra are weakly amphicoelous and strongly crushed transversely, resulting in a deep, narrow morphology that is not representative of their original shape. The centra are only weakly constricted along the middle, giving them a subrectangular shape in lateral view. A shallow ventral furrow (as described by Yates 2003) is preserved on the ventral surface of the proximal caudal centra MSF 15.8.975 and MSF 15.8.488. From the anterior to the middle caudals, the centra gradually become shallower and longer, accompanied by an increase in the elongation index from 1.1 in the more proximal caudal centrum MSF 15.8.975, to 1.8 in the more distal MSF 15.8.1058.

Distal caudal vertebra: MSF 15.8.371 (Fig. 5E) is a distal caudal, probably approximately at the position of ca25. The neural arch bears a small facet that appears to be a broken-off transverse process. The specimen is prepared from the

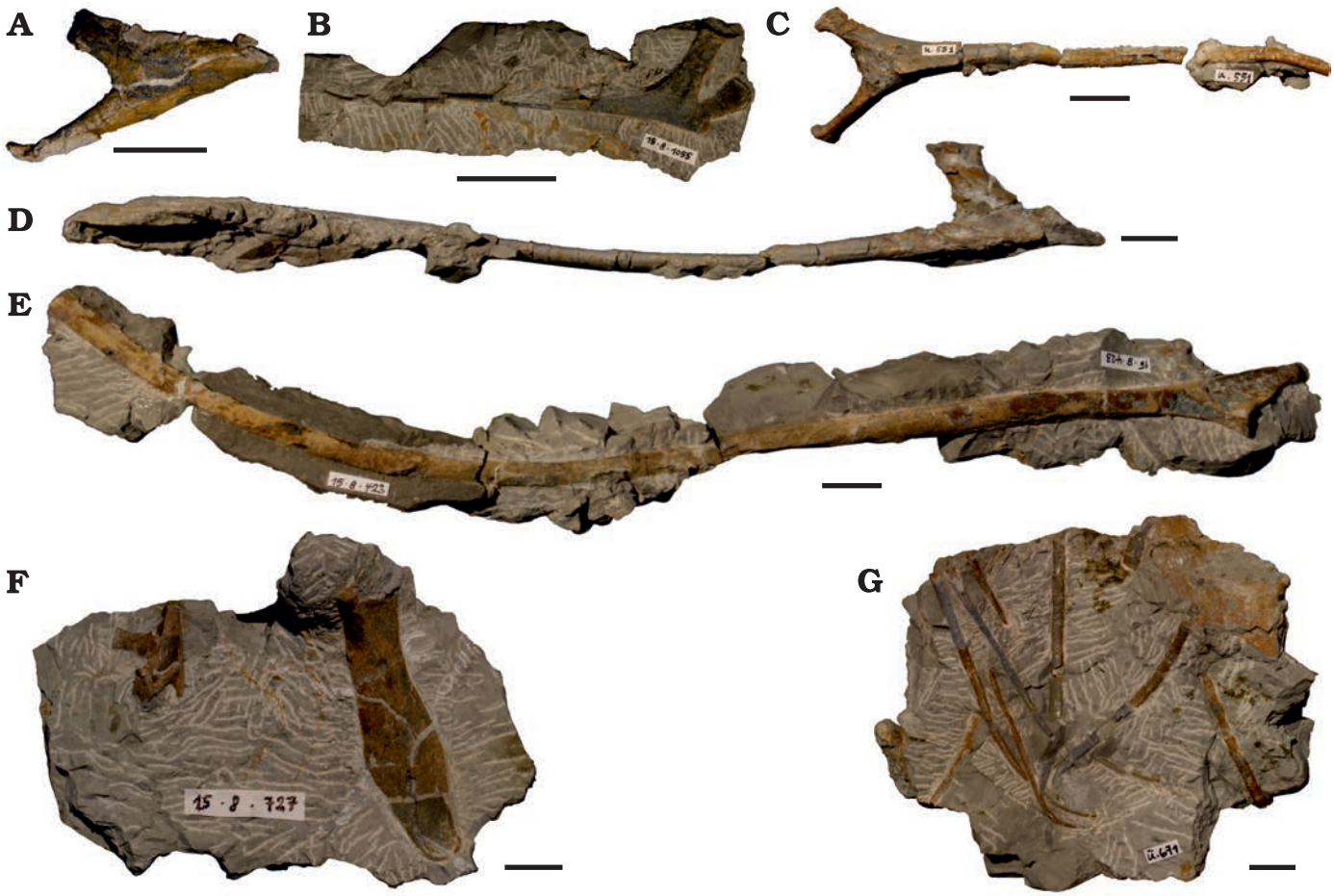

Fig. 6. Ribs of juvenile *Plateosaurus* cf. *trossingensis* Fraas, 1913 skeleton MSF 15.8B. from the Norian of Frick, Switzerland. **A**. Anterior cervical rib, MSF 15.8.2010, in lateral view. **B**. Middle cervical rib, MSF 15.8.1055, in lateral view. **C**. Posterior cervical rib, MSF 15.8.2011, in lateral view. **D**. Anterior dorsal rib, MSF 15.8.384, in anterior view. **E**. Posterior dorsal rib, MSF 15.8.423, in anteromedial view. **F**. Posterior dorsal rib and head of middle cervical rib, MSF 15.8.727, in medial view. **G**. Gastraliae, MSF 15.8.2012. Scale bars 10 mm.

left side and the right side remains in the matrix. The most notable feature of this vertebra is the completely closed and visually indiscernible neurocentral suture, a feature not observed in any other material referrable to "Fabian". Its assignment to the juvenile is hence tentative, because its exact position can not be ascertained, but its small size is within the range expected for its probable position (see Discussion).

The neural spine of this vertebra is very short, shallow and restricted to the posterior extreme of the neural arch, where it is joined by small postzygapophyses. Neither overhangs the centrum, unlike the condition in more anterior caudals. The prezygapophysis is considerably longer, extending anterodorsally and ending in a rounded point beyond the anterior margin of the centrum.

The weakly amphicoelous centrum is elongate, with a length/height-ratio of 1.8 and a very weak central constriction.

Haemal arches: A number of haemal arches preserved with MSF 15.8. (MSF 15.8.531, 785, 726, 1043, 2009) may or may not pertain to the juvenile individual "Fabian", depending on their exact position in the caudal column, which could not be ascertained.

The preserved haemal arches vary in length between 50 and 80 mm. Their articular facets are saddle-shaped and consistently 50–70% wider transversely than they are long anteroposteriorly. The transversely flattened haemal processes have varying levels of anteroposterior expansion at their distal ends, ranging from only a barely perceptible expansion in MSF 15.8.726 to the marked spatulate shape of MSF 15.8.2009.

Cervical ribs: There are three preserved cervical ribs, all characterised by small size (SOM: table S2), slender shafts and the distinctive morphology of their articular ends.

The most anterior one (Fig. 6A) is a rib from the right side (MSF 15.8.2010). The lateral side is strongly convex, while the medial side is concave. The articular end is strongly recurved, so that the capitulum is the anteriormost point on the rib, while the tuberculum is deflected back posterodorsally. The articular region takes the shape of a small, flat plate, from whence the rib gradually narrows towards the shaft, whose distal portion is missing.

MSF 15.8.1055 (Fig. 6B) is a right mid-cervical rib, probably pertaining to c5 or c6. The fairly straight shaft of this rib is preserved, despite being extremely gracile, albeit

fractured into several pieces, which are prepared from the lateral side. The rib is double-headed, with the tuberculum being the longer of the two articular ends. A shallow groove is visible on the lateral side of the base of the tubercle. A small, incompletely preserved anterior process extends beyond the bases of the articular heads. From the broader articular end, where the diameter of the rib is ca. 6 mm, the shaft gradually tapers over a length of 68 mm towards the tip, where the diameter is only ca. 0.4 mm

MSF 15.8.2011 (Fig. 6C) consists of several fragments of a posterior cervical rib. The articular end assumes an almost perfectly symmetrical Y-shape, with the tuberculum and capitulum emanating at the same angle. One of these processes is slightly thicker than the other and is here assumed to constitute the tuberculum, leading the rib being tentatively assigned to the left side. On the proximal lateral portion of the shaft, a low central keel demarks the midline between the articular processes. Two shaft fragments of relatively uniform width are preserved, but the fracture surfaces do not fit together and their correct articulation sequence could not be determined.

Dorsal ribs: A total of 12 dorsal ribs are preserved, the majority from the left side. Only the probable 13th dorsal ribs (Fig. 6E) are preserved from both sides. Most ribs are missing the distal portions of their shafts, and recorded rib lengths refer to the preserved portions of the shaft only. Ribs in "Fabian" are relatively small and gracile, their diameter never exceeding 15 mm (see SOM: table S2). The longest preserved rib (MSF 15.8.871) measures 290 mm from the tubercle to the preserved end of the shaft, but might have been slightly longer when complete.

Anterior dorsal ribs (MSF 15.8.886, right; MSF 15.8.521, left; MSF 15.8.384, left; MSF 15.8.676, left) are characterised by a long tuberculum and strongly angled capitulum. In these ribs, the tuberculum represents the straight continuation of the shaft, whereas the capitulum is directed ventromedially. In its most extreme expression in specimen MSF 15.8.384 (Fig. 6D), the angle between capitulum and tuberculum exceeds 90°, with the capitulum thus pointing slightly distally. The axis between these two facets would have been close to vertical, especially in the anterior three dorsals, where the parapophyses are situated just below the diapophyses on the centrum or at the neurocentral juncture. The shafts of these anterior ribs are mediolaterally flat, with expanded, spatulate ventral ends. The most extreme development of this condition is again observed in MSF 15.8.384.

In middle (MSF 15.8.977, left; MSF 15.8.871, left; MSF 15.8.822, left) and posterior (MSF 15.8.976, shaft only; MSF 15.8.676b, right; MSF 15.8.423, left; MSF 15.8.891, left) dorsal ribs, the tuberculum gradually decreases in size, while the angle of the proximal rib ends becomes flatter. In articulated skeletons, the change in the angle of the capitulum occurs quite abruptly between the fourth and fifth dorsal ribs, whereas the decrease in prominence of the tubercle going posteriorly is more gradual. This is paralleled in the morphology of the vertebrae, where the parapophysis migrates from the dorsal rim of the centrum in the anteriormost dorsals, through an intermediate position at the neurocentral suture ventral to the diapophysis, to a position mostly anterior to the diapophysis. The rib in these vertebrae thus emanates from the parapophysis to contacts the diapophysis dorsally, from where it curves ventrally. The rib shafts become thinner and less flattened, but they remain ovoid in cross-section, the greatest diameter now being in line with the long axis of the articular ends.

The posteriormost dorsal rib preserved in "Fabian", MSF 15.8.727 (Fig. 6F) is tentatively identified as d14 or 15. It differs markedly from more anterior ribs in its short, wide shaft (at a length of 47 mm, and a maximum width of 14 mm). Unlike preceding ribs, the articular end is a short, slightly expanded surface from which anteriorly a short, stout capitulum emanates, with a small facet on the posterior end probably representing the tubercle.

The same slab of matrix preserving this rib also contains the isolated articular end of a cervical rib (cf. c8).

Isolated caudal rib: MSF 15.8.1055 is an isolated, unfused caudal rib, pertaining to one of the proximal caudal vertebrae based on its overall size and large anteroposterior width.

Gastraliae: 15.8.2012 (Fig. 6G), a slab of bone containing 9 gracile bony elements, represents the remains of the gastral basket. The three thinnest elements, with a diameter of less than 1.4 mm, taper to acute, curved points, and are interpreted as medial gastraliae, because these are the most gracile elements in the gastral basket of this taxon (Fechner and Gößling 2014). The remaining bones are shaft fragments of larger lateral gastral elements, with their diameters ranging from 1.4 mm to 2.4 mm.

Appendicular skeleton: Scapula: The scapulae (Fig. 7A, B, SOM: table S3) are elongated bones that are gently arched in the mediolateral plane. Clear differences in width and degree of curvature are present between the left (MSF 15.8.551) and right scapula (MSF 15.8.870) as a result of deformation. The long axis of the scapula is herein treated as vertical for the sake of simplicity.

The scapula has marked expansions both dorsally and ventrally, with the narrowest point being situated ca. 40% from the ventral end, where the width is approximately 13% (left) and 9% (right) of greatest length. The dorsal expansion reaches an anteroposterior width of 53 mm (left) and 38 mm (right), corresponding to 30% and 21% of maximum length respectively. The bone is widest ventrally, measured through the flat, rounded acromial process, where its width reaches almost three times that at the narrowest point, 41% and 32% of greatest length for the left and right scapulae respectively. The right scapula is consistently anteroposteriorly narrower but mediolaterally wider than its left counterpart, as well as more strongly curved, which can be attributed to the different directions of diagenetic deformation suffered by these bones (mediolateral for the left, anteroposterior for the right scapula). The dorsal margin of the acromion emanates at an angle of approximately 50° on the left scapula (ca. 20° on the right, where it is affected by compaction).

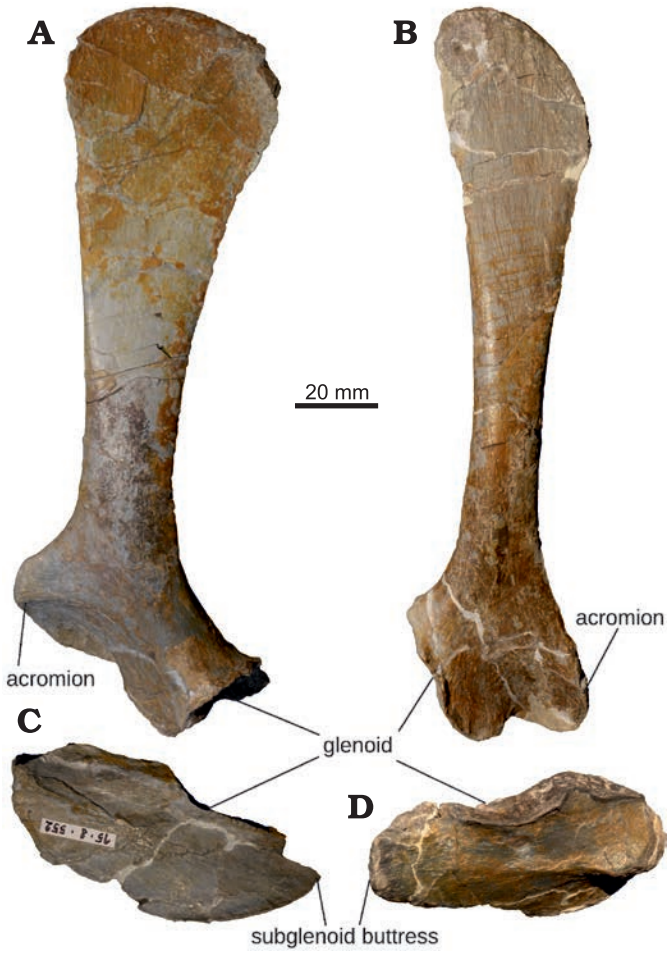

Fig. 7. Pectoral girdle of juvenile *Plateosaurus* cf. *trossingensis* Fraas, 1913 skeleton MSF 15.8B. from the Norian of Frick, Switzerland. **A**. Left scapula, MSF 15.8.55. **B**. Right scapula, MSF 15.8.870. **C**. Left coracoid, MSF 15.8.552. **D**. Right coracoid, MSF 15.8.1035. All in lateral (external) views.

The dorsal scapular end is thin, rounded and paddle-shaped. The right scapula displays a striated surface texture, that is most marked at the proximal expansion and near the glenoid articulation. This texture is less well-preserved on the left scapula. While the scapular blade is mediolaterally thin and flat, especially dorsally, the ventral portion (caput scapulae) is mediolaterally expanded at the glenoid and the coracoid articulation and concave medially. A weakly developed preglenoid ridge curves caudoventrally from the apex of the acromial process, forming the dorsal margin of a shallow preglenoid fossa. The subrectangular glenoid facet is the mediolaterally widest portion of the scapula, and it is delimited by a well-developed lip-like dorsal margin.

Coracoid: The coracoid (Fig. 7CD, SOM: table S3) is of an elongate, subovoid shape, being roughly 2.3 times as long anteroposteriorly as it is wide dorsoventrally. It is laterally convex and medially concave, with prominent margins on its medial side. A short longitudinal ridge runs along the anterior half of the bone. The glenoid facet of the coracoid is more elongated. Resembling the condition on the scapula, the ventral margin of the glenoid is well-defined.

The left and right coracoids differ slightly in overall shape, with the subglenoid buttress (sensu Langer et al. 2007) of the right coracoid (MSF 15.8.1035) being more rounded, whereas that on the left side (MSF 15.8.552) is more tapered. The anterior ridge is better-preserved on the right coracoid. Fine striations are preserved on the right coracoid, most prominently on the subglenoid buttress. No coracoid foramen is present. This feature is variable in other Frick *Plateosaurus* material, and it is unclear whether it is a result of the contained blood vessel invading the bone later in ontogeny, or a mere preservational artifact.

Humerus: Both humeri (Fig. 8A, B; SOM: table S4) are preserved. The left humerus (MSF 15.8.520) is compacted longitudinally and 10% shorter than its counterpart (MSF 15.8.825), giving it a much more robust shape. The humerus is weakly sigmoidal in lateral view. The proximal and distal ends of the humerus are anteroposteriorly flat but mediolaterally expanded compared to the shaft. The proximal end is bent slightly backwards and the distal articular end rotated counterclockwise (as seen in distal view) relative to the proximal expansion. Hence the radial condyle is placed anteromedial to the ulnar condyle. The articular surface of the humeral head is flat, indistinct and forms the medial, proximal corner of the bone. The lateral edge near the proximal surface is folded anteriorly, forming the deltopectoral crest, which has a rounded shape as seen in lateral view (in the less deformed right humerus) and runs along approximately a third of the entire humeral length. It is relatively shorter and lower than in adults, but is still well developed. The distal condyles are flat and only separated by a weak anteroposterior constriction. The angle of torsion between proximal and distal expansions is ca. 30°. Compared to the femur, the humerus is relatively shorter and more gracile than in adult individuals (e.g, von Huene 1907–1908, 1926; Klein and Sander 2007; see SOM: table S6).

Radius: Both radii are preserved (Fig. 8C$_1$, D), with the left (MSF 15.8.526) being compacted in the same manner as the humerus of the same side, rendering it significantly shorter than its right (MSF 15.8.680) counterpart (see SOM: table S4). The bone shaft is almost round in cross-section. Both ends are expanded relative to the shaft, bearing flat, elliptical articular facets with a pronounced rim. In contrast to adult individuals, a biceps tubercle is absent.

Ulna: Only the left ulna (MSF 15.8.525, Fig. 8C) is preserved. The cross-section of the expanded proximal end is triangular, with the anterolateral side being concave proximally for articulation with the radius. The ulna is compacted longitudinally in the same manner as the left radius and humerus, giving it an unnaturally stout shape. The proximal articular surface is only very weakly concave and delimited by a sharp rim. The distal portion is anteroposteriorly flat and expanded to ca. 30 mm in width. The convex distal surface is wide and anteroposteriorly thin. Its cross-section is elliptical. A distinct olecranon process is absent, but the posterior rim of the articular surface is proximally expanded.

Fig. 8. Humerus and antebrachium of juvenile *Plateosaurus* cf. *trossingensis* Fraas, 1913 skeleton MSF 15.8B. from the Norian of Frick, Switzerland. **A**. Right humerus, MSF 15.8.825, in lateral (A_1), anterior (A_2), medial (A_3), and posterior (A_4) views. **B**. Left humerus, MSF 15.8.520, in lateral (B_1) and anterior (B_2) views (note effects of compaction). **C**. Left radius, MSF 15.8.526 and ulna, MSF 15.8.525, in lateral view (C_1) and left ulna, in anterior view with radius not shown (C_2). **D**. Right radius, MSF 15.8.680, in lateral view.

Manus: The manus (Fig. 9) is proportionately long, with the summed length of the longest metacarpal and digit (digit II, SOM: table S6) reaching approximately 80% of the length of the humerus. Up to six ossified carpals, including a radiale and ulnare, have been reported in *Plateosaurus.* However the proximal carpals are usually not preserved

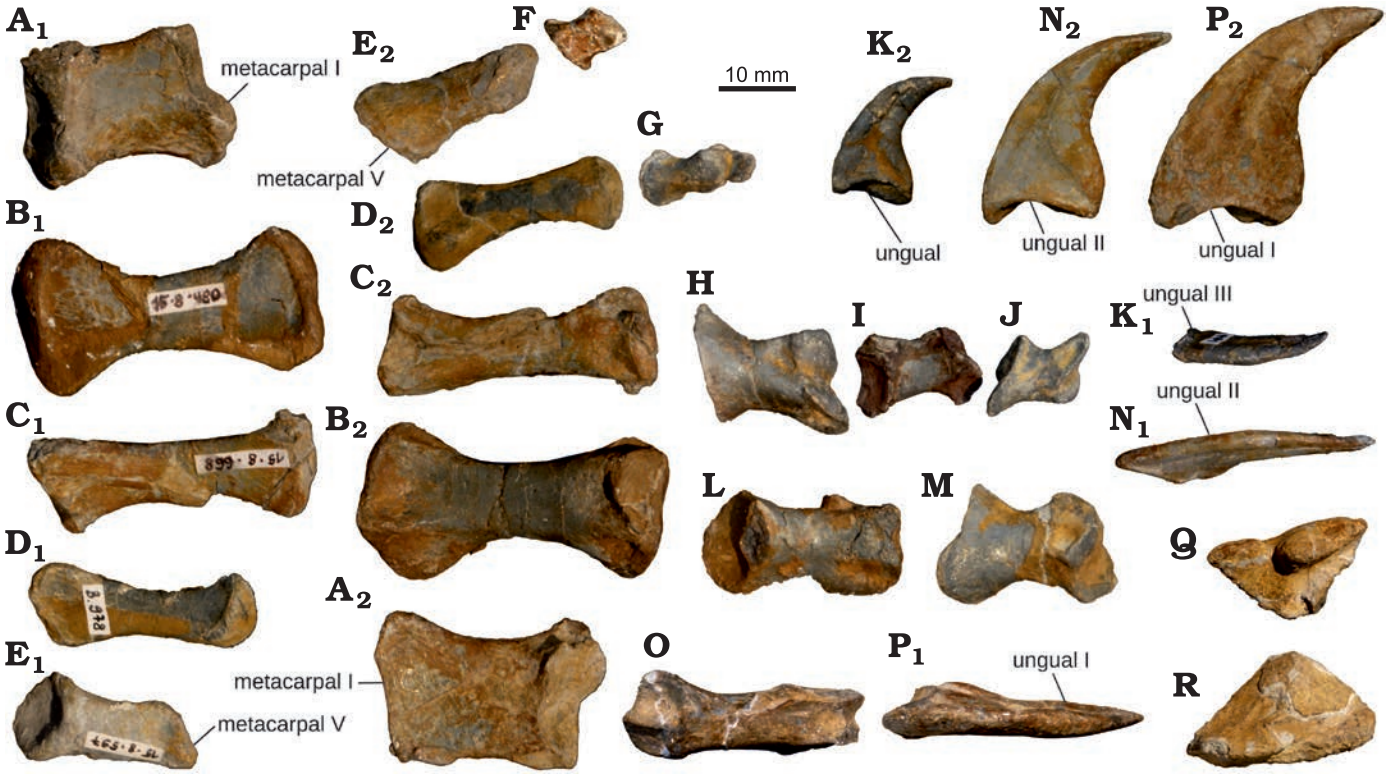

Fig. 9. Manus of juvenile *Plateosaurus* cf. *trossingensis* Fraas, 1913 skeleton MSF 15.8B. from the Norian of Frick, Switzerland. **A**. Left mc I (MSF 15.8.2032). **B**. Left mc II (MSF 15.8.480). **C**. Left mc IIII (MSF 15.8.668). D. Left mc IV (MSF 15.8.2033). **E**. Left mc V (MSF 15.8.597). In palmar (medial) (A_1–E_1) and dorsal (lateral) (A_2–E_2) views. **F**. Left p V-1 (MSF 15.8.671). **G**. Left p IV-1 (MSF 15.8.2014) and p IV-2 (MSF 15.8.2015). **H**. Left p III-1 (MSF 15.8.1077). **I**. Left p III-2 (MSF 15.8.677). **J**. Left p III-3 (MSF 15.8.481). In dorsal (lateral) view (F–J). **K**. Left u III (MSF 15.8.2018), in dorsal (lateral) (K_1) and anterior (preaxial) (K_2) views. **L**. Left p II-1 (MSF 15.8.489). **M**. Left p II-2 (MSF 15.8.477) in dorsal (lateral) view (L, M). **N**. Left u II (MSF 15.8.2017), in dorsal (lateral) (N_1) and anterior (preaxial) (N_2) views. **O**. Left p I-1 (MSF 15.8.467), in dorsal (lateral) view. **P**. Left u I (MSF 15.8.2016), in dorsal (lateral) (P_1) and anterior (preaxial) (P_2) views. **Q**. Right distal carpal I (MSF 15.8.2013). **R**. Right distal carpal II (MSF 15.8.406). In proximal view (Q, R).

(e.g., von Huene 1926; Mallison 2010a), which has led some to suggest that they were cartilaginous (Van Heerden 1997; Remes 2008). No proximal carpals could be reliably identified for MSF 15.8B., which might imply that these bones had not ossified yet.

The right distal carpal I (Fig. 9Q, MSF 15.8.2013) is a flat plate with a roughly triangular outline in proximal and distal aspect. The longest (lateral) edge is 21 mm long in radio-ulnar direction, the dorsopalmar width of the element is 11 mm. The dorsal edge is thickened and a long, low proximal ascending process lines the radial half. On the ulnar side, a shallow furrow separates this process from the rest of the bone, which gradually thins out towards the edges. The distal surface is irregular, bearing a shallow concavity in the middle.

A probable right dc II (Fig. 9R, MSF 15.8.406) is also roughly triangular in proximal view, but has a more rounded ulnar corner than dc I and is slightly larger, with the greatest length reaching 24 mm. The dorsal margin is straight, meeting the radiopalmar margin in an acute point. This margin is the thickest portion of the bone, and it is lined by a short crest anteriorly. Both surfaces bear a light concavity.

Three small bone fragments (MSF 15.8.490) probably constitute remnants of other distal carpals, but none are sufficiently complete or distinct to permit a reliable identification.

All metacarpals of the left manus (Fig. 9A–E) are preserved, while the right manus is missing mc V. In general, the phalangeal formula in *Plateosaurus* is 2/3/4/3/3, with the terminal phalanges of the first three digits being claw-bearing unguals (von Huene 1926). The left manus is more complete, preserving complete digits I–III and partial digits IV and V. The right manus likewise preserves complete digits I and III, partial digits IV–V, and is missing digit II. All three claw-bearing unguals are preserved on both manus.

Proximally, each metacarpal overlaps its ulnar adjacent metacarpal on the oblique, dorsoradially directed anterior surface. Mc I–III articulate in parallel to each other, while mc IV and mc V are abducted (Reiss and Mallison 2014).

Mc I is short and stout (proximal width/total length ratio ca. 0.6), roughly rectangular in dorsal and palmar view, and with a flat rectangular cross-section. Subsequent metacarpals are successively more slender, excepting mc V, which is more robust than mc IV.

In mc I, the grooved articular surface is tilted dorsoradially rather than facing purely distally. The posterior distal condyle is much more prominent than the anterior condyle. The neutral posture of the articulated digit is hence abducted

from the remaining digits in neutral posture. In subsequent metacarpals, the distal articular surface is only weakly grooved (II–III) to fully convex (IV–V). The proximal articular surfaces are weakly convex in mc I–IV, but concave in mc V (see Fig. 9E), differing from adult *P. engelhardti* (sensu Yates 2003), where the proximal end of mc V is flat.

The length gradually diminishes from that of mc II (the longest metacarpal) to roughly half its length in mc V (see SOM: table S4). Mc II–IV are progressively more slender, and have more constricted midshaft sections and trapezoid terminal cross-sections. While their dorsal surfaces are weakly convex, the palmar surfaces are lightly concave, with rims formed by the margins of the articular ends. Unlike in SMNS 13200, no thickened bulge of the shaft is present proximal to the articular groove of mc II. Mc I–III bear anterior pits on the distal articular ends.

Digit I, made up by a single non-ungual phalanx and a large, trenchant ungual, displays the most massive bone structure, while subsequent digits are more slender. There is very little torsion between the articular ends of pI-1, partly due to the radioulnar compaction of this bone. The concave proximal articular surface of this phalanx is traversed centrally by a dorsopalmar ridge, which fits into the intercondylar sulcus of the metacarpal. On subsequent digits, these ridges become less prominent and then disappear, in accordance with the distal surfaces of the corresponding metacarpals. All more distal phalanges are proximally convex, with a central ridge to fit the grooved distal articular surfaces of more proximal phalanges, with the dorsal rim overhanging significantly.

The ungals (Fig. 9K, N, P) present on the first three digits are strongly compressed in radioulnar plane. Their size and robustness gradually diminishes in ulnar direction. The proximal articular facets are tall in dorsopalmar direction and saddle-shaped. The flexor tubercles of the unguals are small, but more prominent than on the pedal unguals. Their outer curvature remains relatively uniform, while the inner curvature is weak in ungual I and increases towards ungual III.

Ilium: Both ilia (Fig. 10A, B) are preserved, but heavily affected by compaction (see SOM: table S3). In the left ilium (MSF 15.8.717), the axis of compaction appears to have been primarily mediolaterally oriented, resulting in flattening. In the right ilium (MSF 15.8.486) on the other hand, this axis is directed from anterodorsal to posteroventral, resulting in a significantly shortened iliac blade. Two weakly defined ridges are present on the medial surface, extending anteroventrally from the posterior corner and horizontally from the anterior corner of the blade. The lateral surface is weakly concave, delimited by the brevis shelf and supraacetabular crest ventrally and by the lateral eminences of the pre- and postacetabular processes. Fanned striations mark the preacetabular process and dorsal portion of the postacetabular process. The weakly convex dorsal margin is interrupted by a small indentation offsetting the preacetabular process from the rest of the blade. The medially open acetabulum is bordered anterodorsally by a prominent supraacetabular crest that continues onto the long, straight pubic peduncle. The shorter ischial peduncle is broader and flatter than the pubic peduncle and lacks a crest. Its ventral end forms a widened posterior heel. The preacetabular process is short and subtriangular, and does not extend anteriorly to the anterior margin of the pubic peduncle. The postacetabular process is much longer and bears a pronounced posterior mediolateral swelling. Posteriorly, its ventral surface is concave, forming the brevis fossa, which opens up anterolaterally onto the ventrolateral surface of the postacetabular process. The fossa is bounded by lateral and mediolateral brevis shelves, running from the ventral part of the postacetabular process towards the base of the ischial peduncle (Fig. 10A, B), as is characteristic for *Plateosaurus* and *Ruehleia* (Rauhut et al. 2020). In lateral view, the posterior corner of the postacetabular process is rounded in the left ilium (MSF 15.8.717), but deformation on the right side gives the appearance of a more angular morphology.

Pubis: Only the right pubis (MSF 15.8.383) is preserved (Fig. 10C). The shaft is a roughly parallel-sided plate that is dorsoventrally very thin throughout most of its length, the thickest portion being the rounded lateral rim. The distal end of the shaft is anteroposteriorly thickened. The obturator plate is very thin and angled posteriorly (counterclockwise in dorsal view) from the shaft by ca. 40°. It encloses a large obturator foramen shaped like a strongly rounded triangle as well as a small ventrolateral accessory foramen. The lateral edge of the shaft bears a lightly convex scar approximately 15 mm long in proximodistal direction, corresponding in its position to the pubic tubercle described by Yates et al. (2003), but very weakly developed. The iliac and pubic articulations at the proximal end are thickened anteroposteriorly.

Ischium: Both ischia (MSF 15.8.421) are preserved in articulation but remain separated by a well-discernable suture line (Fig. 10D). The obturator plate of the ischium is very broad anteroposteriorly. Its proximal margin bears two widened facets for articulation with the ilium dorsally and the pubis anterodorsally. The articular facets are separated by a transverse constriction in the ischial rim. In proximal aspect, the ischium is butterfly-shaped. The posterior ischial facets are wider and spaced further apart than the more rounded anterior expansion for articulation with the pubis. The iliac facet is almost triangular in shape, while the pubic facet is narrower and more scythe-shaped. Both facets are slightly angled dorsolaterally. In lateral view, the obturator plate abruptly narrows and is separated from the shaft by a nots, as described by Yates (2003) for *P. engelhardti*, but the anteroposteriorly narrow shafts are firmly appressed and a medial fenestra is not discernable. Their distal heel faces posteriorly, which might be a result of deformation.

Femur: Both femora (Fig. 11A, B, SOM: table S5) are preserved, showing considerable morphological differences as a result of compaction. The right femur (Fig. 11B, MSF 15.8.380) is sigmoidal in anterior and posterior view,

Fig. 10. Pelvic girdle of juvenile *Plateosaurus* cf. *trossingensis* Fraas, 1913 skeleton MSF 15.8B. from the Norian of Frick, Switzerland. **A**. Left ilium, MSF 15.8.717, in lateral (A_1) and medial (A_2) views. **B**. Right ilium, MSF 15.8.486, in lateral (B_1) and medial (B_2) views (note differences due to effects of compaction). **C**. Right pubis, MSF 15.8.383, in lateral (C_1) and anterior (C_2) views. **D**. Articulated ischia, MSF 15.8.421, in posterior (D_1) and right lateral (D_2) views.

whereas the left femur (Fig. 11A, MSF 15.8.565) appears relatively straight. The left femur is more arched in the parasagittal plane, while the right femur appears completely straight in lateral view. The ratio of anteroposterior to mediolateral diameter at midshaft is ca. 1.7 in the left femur, whereas it is 0.6 in the right femur.

The same differences due to compaction can be observed in the proximal and distal surfaces. The left femoral head is greatly shortened mediolaterally and the medial surface is flattened so that the greatest distal diameter is through the tibial condyle, as opposed to the fibular condyle in the right femur. The femoral head points directly medially, forming a

Fig. 11. Femur, tibia, fibula, and proximal tarsus of juvenile *Plateosaurus* cf. *trossingensis* Fraas, 1913 skeleton MSF 15.8B. from the Norian of Frick, Switzerland. **A**. Left femur, MSF 15.8.565, in medial (A_1), anterior (A_2), lateral (A_3), posterior (A_4), proximal (A_5), and distal (A_6) views. **B**. Right femur, MSF 15.8.380, in lateral (B_1), anterior (B_2), and proximal (B_3) views (note different effects of compaction). **C**. Left tibia, MSF 15.8.381, in anterior (C_1), lateral (C_2), medial (C_3), proximal (C_4), and distal (C_5) views. **D**. Left fibula, MSF 15.8.518, in lateral (D_1) and medial (D_2) views. **E**. Right calcaneum, MSF 15.8.469, in proximal view. **F**. Right astragalus, MSF 15.8.585, in proximal (F_1) and anterior (F_2) views. **G**. Left astragalus, MSF 15.8.420, in proximal (G_1) and anterior (G_2) views.

horizontal proximal surface with a shallow central groove. Near the articular ends, the anterior, lateral and posterior surfaces of the femur are striated. The lateral margin of the proximal end is formed by a flat greater trochanter. The cranial trochanter (sensu Galton and Upchurch 2004 = trochanter major of von Huene 1926 = lesser trochanter of Langer et al. 2019) is a rounded, slightly curved crest rising from the anterior surface of the femur; it is well-preserved in the left femur, but broken off in the right. The fourth trochanter is very well developed, forming a crest along the central posterior surface of the bone, starting ca. 70 mm from the proximal extreme of the bone and with a proximodistal length of ca. 50 mm. The thinnest point of the shaft is situated just below it. Anterior to the fourth trochanter, the medial surface of the femur bears an ovoid muscle scar.

The distal end of the femur curves backwards in the left femur, but laterally in the right femur, and the plane of greatest distal diameter is anteroposterior in the left femur, but mediolateral on the right side. The medial (tibial) and lateral (fibular) condyles are separated by a deep sulcus that extends onto the posterolateral surface of the shaft. Anteriorly, the condyles meet to form a thick rim enclosing the intercondylar concavity. The fibular condyle is offset from the lateral surface of the shaft by a shallow groove.

Tibia: Only the left tibia (MSF 15.8.381) is preserved (Fig. 11C, SOM: table S5). It is straight, mediolaterally compacted and slightly shorter than the femur. The dorsal articular end is marked by a strong anteroposterior expansion. The mediolateral expansion is less marked as a result of compaction. In proximal aspect, the head appears almost triangular in outline, with a more concave lateral and flat medial side. The proximal surface is flat and steeply sloped laterally. The cnemial crest is weakly developed. The cross-section at midshaft is elliptical, with an aspect ratio (anteroposterior/mediolateral) of 1.7, closely matching the corresponding femur. The distal end is slightly expanded and bears a small descending process (processus distalis posterior or malleolus tibiae of von Huene 1926) which points distally and slightly anterolaterally. The anterior part of the distal articular surface is flat, and separated from the posterior process by a small concavity that continues onto the lateral surface as a groove, excavating the distal part of the bone. The medial part of the distal surface is convex.

Fibula: The left fibula (Fig. 11D, SOM: table S5, MSF 15.8.518) is a long, very gracile bone with slightly widened ends, which are set at an angle of ca. 45° from each other. The entire bone is slightly arched, the convex side facing laterally, and the proximal portion additionally curves slightly posteriorly.

Unlike in adult individuals, the fibula is slightly shorter than the tibia, but this might be the result of a minor degree of compaction. In proximal view, the fibula is mediolaterally flat and roughly semilunar in outline. The medial side of the proximal end is markedly concave for ca. 40 mm, below which the shaft cross-section becomes elliptical. The concavity is delimited by prominent rims. A narrow groove runs for another 85 mm down the posteromedial side of the fibular shaft. The distal end has a more elliptical cross-section and is mediolaterally thicker than the proximal end.

Pes: Both astragali are preserved (Fig. 11F, G, SOM: table S5), the right one (MSF 15.8.585) more complete than the left one (MSF 15.8.420). In dorsal view, it is wing-like in outline, with a broad, dorsally concave medial portion that terminates in a rounded anteromedial corner, with a convex posteromedial edge. The base of the ascending process runs mediolaterally along the middle of the bone for ca. 18 mm. No foramina are discernible here, however adhering matrix and poor preservation partially obscure anatomical details of this region. The greatest proximodistal thickness of the astragalus, at the anteromedial apex of the ascending process, reaches 17 mm. Laterally, the fibular articulation is formed by a small, slightly concave facet. The entire distal surface is moderately convex.

The right calcaneum (Fig. 11E, MSF 15.8.469) is a thick, subrectangular plate, 21 mm long anteroposteriorly and 14 mm wide. The proximal surface is bisected by a ridge running parallel to the curved medial edge. The distal face and sides of the bone remain obscured by adhering matrix.

A small, irregular-shaped plate is preserved proximal to mt II on the slab containing the articulated left pes (Fig. 12A), and is tentatively identified as the corresponding distal tarsal (ta II). The element is flat and weakly convex proximally.

A larger (30 mm by 22 mm), equally flat plate (Fig. 12B, MSF 15.8.823) may be ta-III or IV. It resembles a strongly rounded triangle, with lightly convex and concave distal and proximal surfaces respectively. Two small tubercles are present adjacent to the thickened posterior margin of the plate. The maximum thickness is 4 mm.

Another probable distal tarsal is a small, subrectangular plate (MSF 15.8.420), measuring ca. 18 mm long in dorsoplantar direction and thickening towards one end. The distal surface is marked by a shallow concavity, the dorsal surface is slightly saddle-shaped.

The left foot preserves semi-articulated mt I–IV. The disarticulated right foot is represented by mt II–V. The length is smallest in mt I, markedly longer in mt II and greatest in mt III, before decreasing again in mt IV and V (see SOM: table S5). The proximal articular surfaces of mt I through III are flat, those of mt IV and mt V more convex. The distal articular ends are convex to very weakly grooved (mt III).

Mt I has a proximal width/maximum length ratio of 0.5. The flat plantar surface is firmly appressed to the anteromedial surface of mt II. The widest plane of the bone is hence aligned anteroposteriorly to anterolaterally, with a slight degree of torsion between the proximal and distal articular surfaces. In proximal view, the surface of mt I thins out anteriorly.

In mt II and mt III, the shaft cross-section is roughly rectangular, and the expanded distal articular end bears shallow pits on the lateral and medial surfaces.

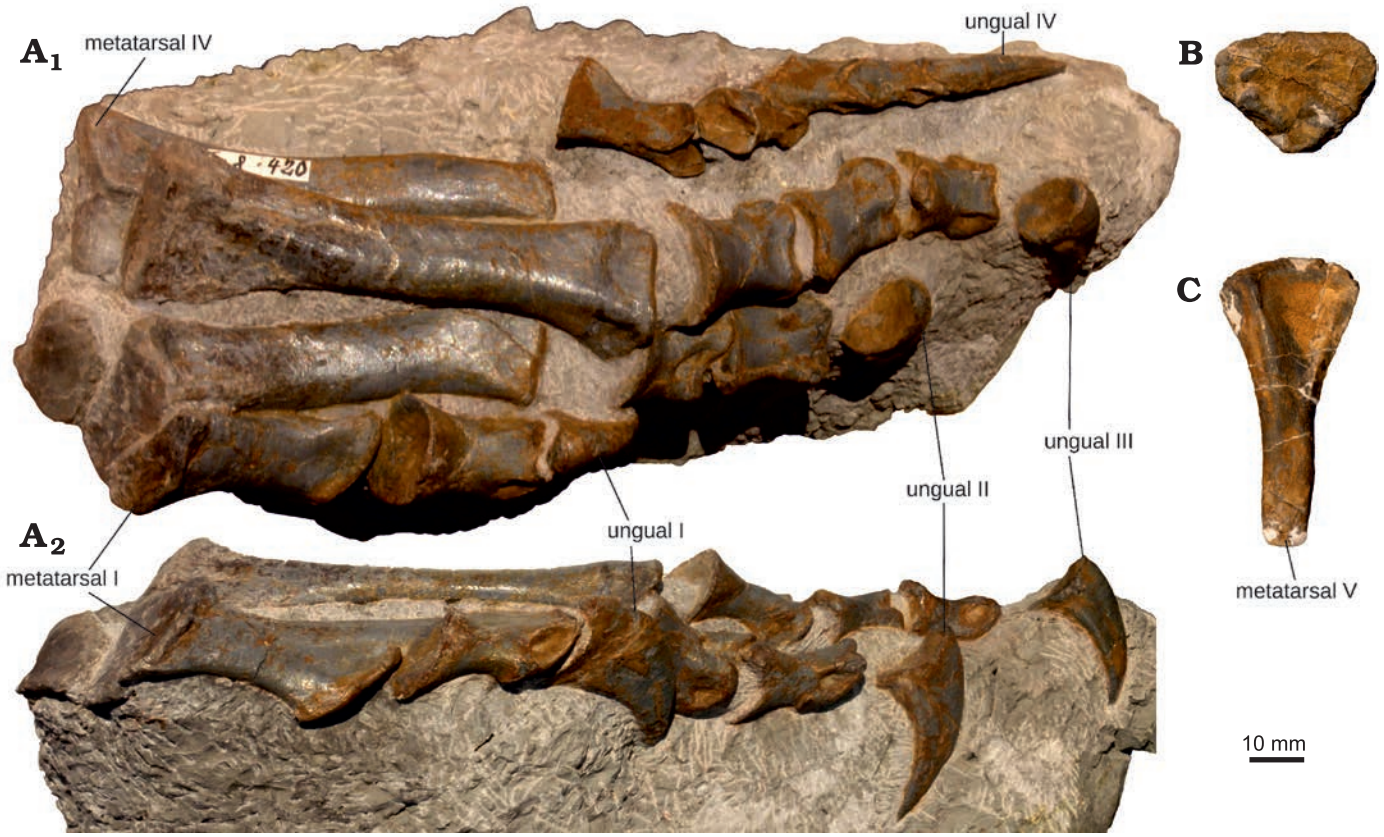

Fig. 12. Pes of juvenile *Plateosaurus* cf. *trossingensis* Fraas, 1913 skeleton MSF 15.8B. from the Norian of Frick, Switzerland. **A**. Left pes, MSF 15.8.2019, in dorsal (A_1) and medial (A_2) views. **B**. Distal tarsal III or IV, MSF 15.8.823, in distal view. **C**. Right metatarsal V, MSF 15.8.826, in dorsal (anterior) view.

Mt IV and mt V (Fig. 12A, C) are progressively flatter and more triangular in proximal-cross-section, with the distal expansion absent and the articular surface small and convex. Each metatarsal articulates and overlaps with posterolateral surface of the preceding one.

The phalangeal formula in *Plateosaurus* is 2/3/4/5/3, the inner four toes terminating in claw-bearing unguals (Mallison 2010a; von Huene 1926). The phalanges are mostly preserved, the left foot being more complete than the right. Digits I–III are fully preserved and articulated. A mostly articulated digit IV is also present, but was not found in articulation with the rest of the pes. The left foot preserves digits I–III. The phalanges of the left foot are generally more affected by compaction, giving them a short, flat appearance, while those of the right foot are deeper and longer. Digit V is not preserved.

At the proximal metatarsophalangeal joints, all phalangeal articular surfaces are strongly convex. In more distal phalanges, the proximal articulations are saddle-shaped and have medially strongly overhanging dorsal and plantar margins, while the distal ends are grooved and bear pronounced pits on the medial and lateral surfaces. The more distal phalanges very gradually diminish in size.

Four pedal unguals of the left and three of the right foot are preserved. These are heavily affected by deformation, so that their original shape is difficult to discern. While they are similar to the manual unguals in size and joint morphology, they appear to have been less laterally compressed and straighter than the manual unguals, in accordance with other *Plateosaurus*-specimens, and do not bear the same pronounced flexor tubercles as the manual unguals.

Body size.—Due to its relative completeness, "Fabian" lends itself to several methods of body size estimation. Femur length has previously been used as a proxy for body size (e.g. Sander 1992; Hofmann and Sander 2014). At 240 mm (see Tables 1, 2, SOM: table S6), the femur of "Fabian" is approximately half the length of the smallest previously known femora of *Plateosaurus* (Klein and Sander 2007; Hofmann and Sander 2014). This also applies to the estimated femur lengths of previously described juvenile material from Frick (Hofmann and Sander 2014). Based on the ratio between total length and femur length in GPIT 1 (Mallison 2010a), this suggests a total body length from the tip of the snout to the tip of the tail of ca. 2.3 m.

Based on comparison of vertebral lengths between "Fabian" and SMNS 13200 (see Fig. 13; Hofmann and Sander 2014; von Huene 1926), the neck and trunk length (including the sacrum) of "Fabian" can be estimated at approximately 450 mm and 640 mm respectively (SOM: table S6). Accounting for an estimated skull length of ca. 150 mm (SOM: table S6), the total rostrosacral length can

Table 1. Selected measurements (in mm) of axial skeleton of juvenile *Plateosaurus* cf. *trossingensis* (MSF 15.8B.). Zygapophyseal length is the maximum length between pre- and postzygapophyses projected into the sagittal plane. Centrum length is measured "rim to rim" in a straight line in the sagittal plane on the ventral side of the centrum. Abbreviations: c, cervical vertebra; ca, caudal vertebra; d, dorsal vertebra; s, sacral vertebra.

Bone	Field number	Zygapophyseal length	Centrum length
c2	MSF 15.8.2001	47.8	–
c3	MSF 15.8.669/939	56.7	43.0
c4	MSF 15.8.1032/979	74.5	53.0
c6	MSF 15.8.2002/592	60.4	54.2
c9	MSF 15.8.671/905	59.9	37.1
d1	MSF 15.8.2003	–	28.5
d2	MSF 15.8.908/978	45.4	36.1
d3	MSF 15.8.2004/2005	41.8	26.8
d4	MSF 15.8.477	39.3	–
d5	MSF 15.8.2006	–	–
d6	MSF 15.8.654/906	49.8	36.1
d7	MSF 15.8.1076/437	57.4	32.1
d8	MSF 15.8.885	58.4	–
d9	MSF 15.8.728/679	56.8	32.2
d12	MSF 15.8.468/2007	41.9	30.3
s1	MSF 15.8.558	48.7	–
ca	MSF 15.8.889	45.4	–
ca	MSF 15.8.972	43.7	–
ca	MSF 15.8.476	39.0	–
ca	MSF 15.8.2008	–	–
ca	MSF 15.8.975	–	27.5
ca	MSF 15.8.488	–	29.6
ca	MSF 15.8.1058	–	33.2
ca	MSF 15.8.371	24.9	21.5

hence be estimated at 1.22 m. Including the tail, the resulting total length is 2.31 m, closely matching that estimated from the femur length.

The minimum right femur circumference of "Fabian" (85 mm, eccentricity of 1.7) suggests a body mass of 36 kg (25% prediction error range of 27–45 kg) based on femur circumference (Campione et al. 2014; Campione 2016). Volumetric mass estimates available for specimen GPIT 1 are 600–912 kg (Gunga et al. 2007; Mallison 2010a). At a femur length of 5.95 m (Mallison 2010a), this individual appears to represent a typical-sized adult (Klein and Sander 2007). Isometric scaling based on trunk length (the proportionately longer neck is expected to add little to overall mass based on segment volumes calculated by Mallison 2010a) and femur length suggests body masses of 36–54 kg and 40–62 kg respectively, which is roughly consistent with the range predicted from femur circumference.

Discussion

Taxonomic assignment.—Examination of the material of MSF 15.8B. revealed no major morphological ferences between it and either the type series of *Plateosaurus engelhardti* (and the material assigned to this species from Ellingen, Bavaria) as redescribed by Moser (2003), or the *P. trossingensis* specimens from Frick (MSF 23), and Trossingen (SMNS 13200, GPIT 1 and 2) used for comparison, including the holotype of the latter. However, the type material of *P. engelhardti* does not offer much overlapping material and hence is not a useful standard for comparison, leaving the question of synonymy between *P. engelhardti* and *P. trossingensis* beyond the scope of this work. Notably, since most of the sacrum is missing in MSF 15.8B., it can not be ascertained whether it matches the "Trossingen-type" sacrum as opposed to the *P. engelhardti*-type sensu Galton (2001). MSF 15.8B. closely matches the more complete *P. trossingensis* material that served as the primary standard for comparison, especially in the pattern of laminae and fossae on the vertebrae and the differentiation within the vertebral collumn, as well as the overall morphology of the appendicular skeleton. Where differences are present this is mostly restricted to changes in relative robusticity, not qualitative features. We hence tentatively assign MSF 15.8B. to *P. trossingensis*.

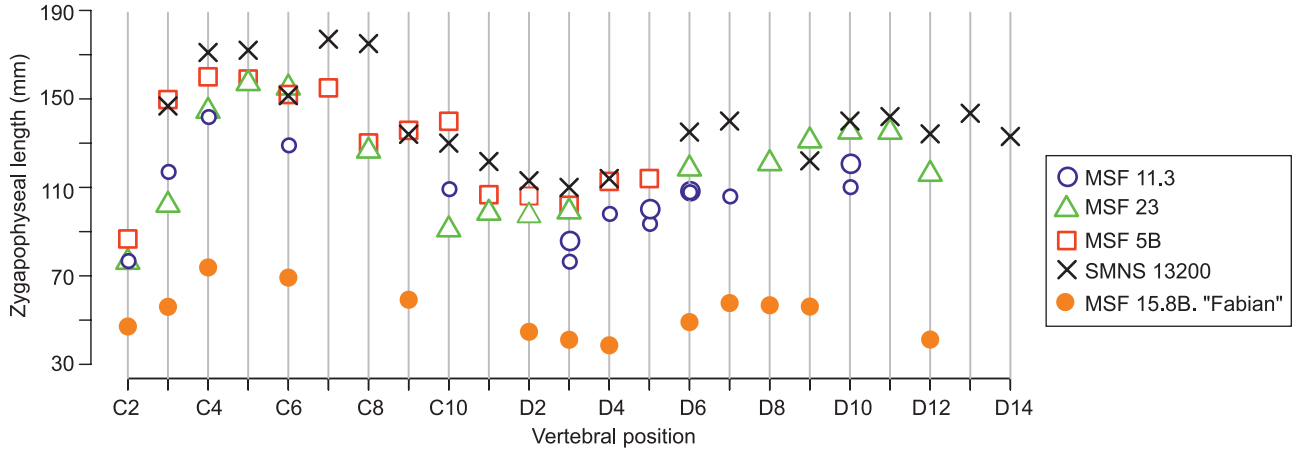

Fig. 13. Comparative plot of zygapophyseal lengths of *Plateosaurus* neural arches. Note size difference between large juvenile (MSF 15.8B.) and adult neural arches described by Hofmann and Sander (2014).

Table 2. Selected measurements (in mm) of appendicular skeleton of juvenile *Plateosaurus* cf. *trossingensis* (MSF 15.8B.). Greatest length is measured in a straight line. Articular lengths are measured between deepest depression or middle of articular surfaces. Medio-lateral widths are measured at midshaft for humerus, femur, tibia and fibula, at the thickest portion for other bones. Abbreviations: L, left; R, right. Phalanges [a] 2 combined non-ungual, [b] ungual, [c] 3 combined non-ungual.

Bone		Field number	Greatest length	Shaft circumference	Articular length	Medio-lateral width
Scapula	R	MSF 15.8.870	179.0			27.8
	L	MSF 15.8.551	177.0			16.6
Ilium	R	MSF 15.8.486	98.8			37.8
	L	MSF 15.8.717	132.7			24.8
Humerus	R	MSF 15.8.825	121.4	52.0		
	L	MSF 15.8.520	109.3	58.0		
Radius	R	MSF 15.8.526	62.2		56.5	
	L	MSF 15.8.680	84.3		70.1	
Ulna	R	MSF 15.8.525	79.5		68.0	
Metacarpal II	R	MSF 15.8.490	41.0		40.0	
Manual digit II	L	MSF 15.8.489/477, 2017	47.6[a] 33.5[b]		32.7[a] 27.8[b]	
Femur	R	MSF 15.8.380	236.0	85.0		31.5
	L	MSF 15.8.565	243.0	76.5		18.5
Tibia	L	MSF 15.8.381	211.0	64.5		14.5
Fibula	L	MSF 15.8.518	195.0	41.0		9.1
Astragalus	R	MSF 15.8.585				58.5
	L	MSF 15.8.420				51.0
Metatarsal III	R	MSF 15.8.420	94.7		82.7	
Pedal digit III	R	MSF 15.8.420	40.4[b] 84.3[c]		34.9[b] 62.3[c]	26.5

Ontogenetic stage.—Based on the morphological similarity of the vertebrae to those of adult individuals of *Plateosaurus*, and the open neurocentral sutures, "Fabian" would correspond to the late juvenile ontogenetic stage (MOS 3) sensu Carballido and Sander (2014). This contrasts with the estimated body size, which suggests that this individual must have been in the early phases of growth.

Compared to adult body size, eggs and hatchlings of *Massospondylus* and *Mussaurus* (Reisz et al. 2005; Otero et al. 2019) are relatively small. Its body size suggests that "Fabian" must have been well beyond the hatchling stage. The ontogenetic stage of "Fabian" is currently being investigated using bone histology which will be described in a future paper.

Preservation.—The fossil material from Frick is more compacted than that from Trossingen and especially Halberstadt (PMS, personal observation). Furthermore, compaction of "Fabian" may be expected to be especially pronounced because of its early ontogenetic stage and concomitant weaker ossification (see Hugi and Scheyer 2012). In keeping with this, almost all the skeletal elements of "Fabian" show some degree of post-mortem deformation, most commonly manifested as transverse or dorsoventral flattening of vertebral centra or neural arches or limb shafts. The more extreme cases of compaction are the left humerus and antebrachium, both femora and ilia, along with the articulated ischia and the left pes. A particularly extreme case is represented by the right ilium, which is shortened by 25% relative to its counterpart (see SOM: table S3). The ilia differ greatly in morphology as a result. Notably, whereas the left ilium displays the typical morphology of *Plateosaurus*, the postacetabular process of the right ilium is squared-off in a manner superficially reminiscent of *Efraasia minor* (Yates 2003).

Such marked differences between some bones of a single individual caused by diagenetic compaction highlight the importance of distinguishing diagenetic artifacts from taxonomically informative characters (Moser 2003) when diagnosing species. This is especially relevant to Galton's (2000) suggestion of distally straight femora as an autapomorphy of *P. engelhardti* and Weishampel and Chapman's (1990) recognition of two femoral morphs in Trossingen, which they suggested might indicate sexual dimorphism. The contralateral femora and ilia of MSF 15.8B. display a strikingly different morphology, which could have led to erroneous recognition of distinct morphs if diagenesis were not considered, similar to the condition described by Moser (2003) for SMNS 13200.

Taphonomy.—MSF 15.8B. ("Fabian") is estimated at less than half the linear dimensions, and ⅛ the body mass of the next-smallest individuals of *Plateosaurus* described (see Hofmann and Sander 2014). A total length of ca. 5 m has previously been suggested as the size limit for *Plateosaurus* to become mired, explaining the absence of smaller individuals in all *Plateosaurus* bonebeds (Sander 1992). By contrast, the juvenile described herein was probably below 2.5 m total length (Fig. 14).

The skeleton was found in a circular bone concentration less than 3 m in diameter, in association with at least five larger individuals. The hindlimbs and tail (MSF 15.8A.) of an adult *Plateosaurus* from the bone concentration that yielded

Fig. 14. Skeletal reconstruction of MSF 15.8B., preserved elements highlighted in white, grey elements restored following adult *Plateosaurus* skeletons SMNS 13200 (von Huene 1926) and GPIT 1 (Mallison 2010a, b).

MSF 15.8B. are preserved in articulation, which is consistent with miring of this individual (Sander 1992). The shape of the bone field suggests that it represents a small-scale mudhole or puddle, where the mud could potentially have been soft enough for even small animals to become mired, whereas the surrounding surface may have been dried out and sufficiently solid for small animals to traverse it. If adult *Plateosaurus* individuals became mired first, their motion in the sediment may have contributed to this liquefaction. Other *Plateosaurus* that became trapped in the same mudhole later on might also have contributed to the disarticulation of the skeleton.

"Fabian" does not represent the first dinosaurian remains below the size of adult *Plateosaurus* to be found at the Gruhalde Quarry, with the partial skeleton of the small (2.6–3.0 m), basal averostran theropod *Notatesseraeraptor* (MSF 06-1 and MSF 09-2) having been discovered at the site in 2006 (Zahner and Brinkmann 2019). However, this material does not come from the same horizon as the *Plateosaurus* bonebeds and thus does not refute the miring hypothesis.

In any case, the rarity of all other dinosaurs compared to adult-sized *Plateosaurus* suggests a significant preservational bias towards large animals, which is generally consistent with the miring hypothesis as proposed by Sander (1992). In this, *Plateosaurus* differs notably from most other dinosaurs, which are often primarily or exclusively known from immature individuals (e.g., Myhrvold 2013).

Growth and development.—The striking morphological similarities between the juvenile and adult specimens of *Plateosaurus* could mean that morphological features generally developed early in ontogeny, or alternatively that there was plasticity in the development of morphology, with some individuals attaining morphologically adult characteristics earlier than others. However, testing this hypothesis would require a larger sample of early juvenile specimens than is currently available.

Due to allometric changes of the forelimbs and axial column during growth, hatchlings and juveniles of the massopods *Massospondylus* (Reisz et al. 2005, 2010) and *Mussaurus* (Otero et al. 2019) were proposed to have been quadrupeds, despite obligate bipedalism in adults (as in *Plateosaurus*, Bonnan 2007; Mallison 2010a; Reiss and Mallison 2014). Recent work suggests that the embryonic *Massospondylus* individuals analyzed by Reisz et al. (2005, 2010) were of an earlier developmental stage than originally thought (Chapelle et al. 2020), calling into question their implications for hatchling morphology and locomotion. However Reisz et al. (2012) describe further corroborating evidence for hatchling quadrupedalism in the form of small-sized manus-pes print sets referrable to *Massospondylus*. Like juvenile *Mussaurus*, but unlike the embryonic *Massospondylus*, the juvenile *Plateosaurus* has proportionately long cervical vertebrae (see SOM: table S6). However, by contrast, the humerus and forearm as preserved are comparatively short, and the proportions appear inconsistent with quadrupedality. This might be partly attributable to compaction, exemplified by the differences in length between both humeri, but the already gracile morphology of the less compacted humerus argues against a strong proximodistal compression in this element. However, since the individual is of considerably greater body size, comparison with embryonic *Massospondylus* (Reisz et al. 2005, 2010) or hatchling *Mussaurus* (Otero et al. 2019) individuals remains of limited utility for assessing the overall ontogeny of *Plateosaurus.*

The inferences that can be drawn about the pattern of suture-closure in *Plateosaurus* from the juvenile described here are limited by the general lack of fusion of its neurocentral sutures. The only exception to this rule is a small, distal caudal vertebra (MSF 15.8.371), whose neural arch is completely fused to the centrum. This calls its referral to "Fabian" into question. However based on the presence of the broken base of a transverse process, the vertebra's position can be constrained to be no more posterior than the 25th caudal position. In SMNS 13200, ca25 has a centrum length of 58 mm, with progressively more anterior vertebrae being larger. The centrum length of MSF 15.8.371 is 21.5 mm. The average length of the juvenile presacral vertebrae is 38% that of the corresponding vertebrae in SMNS 13200 (von Huene 1926), suggesting the 25th caudal centrum should be approximately 22 mm long. The size of MSF 15.8.371 therefore consistent with a referral to "Fabian", suggesting that suture closure in *Plateosaurus* started in the distal tail and progressed

anteriorly. This is also consistent with the pattern of suture closure observed in extant crocodilians (Brochu 1996).

Interestingly, the mid-caudal neural arches also follow a pattern of increased fusion of the caudal ribs from anterior to posterior. Hofmann and Sander (2014) reported circumstantial evidence of suture closure progressing from posterior to anterior, in the form of the absence of unfused posterior dorsal and caudal neural arches. Posteroanterior progression of suture fusion is also found in Sauropoda (Schwarz et al. 2007). Hence, the evidence suggests that the suture closure in *Plateosaurus* started in the distal caudals and then progressed anteriorly, even though multiple centres of early suture-closure are also a possibility.

Pneumatic features.—The strong development of a pattern of laminae and fossae essentially identical to that in adult *Plateosaurus* individuals may have been linked to an avian-style respiratory system. Evidence of such a system has been described for other basal sauropodomorphs, and is expected based on phylogenetic bracketing (Wedel 2006, 2007; Butler et al. 2012). Air sac diverticula develop late in ontogeny in extant birds (Wedel 2009) but the laminae may have played a role in guiding the development of these structures by acting as osseous septa (Schwarz et al. 2007). The presence or absence of pneumosteal bone tissue (Lambertz et al. 2018) might prove useful for assessing the state of development of pneumatic structures throughout ontogeny.

Laminae and fossae in "Fabian" are especially strongly developed in the posterior cervical and anterior dorsal region. This resembles the condition in other *Plateosaurus* individuals and the position of previously reported pneumatic subfossae (Yates et al. 2012) and a probable pneumatopore (Janensch 1947) in posterior cervical vertebrae. It differs from the condition in a juvenile individual assigned to *Barosaurus*, where a pneumatic hiatus in the mid-dorsal region suggests distinct centres of pneumatisation in the anterior and posterior dorsal regions (Melstrom et al. 2016) and more closely resembles the condition in the indeterminate juvenile diplodocid SMA 0009, which is of a similar size and presumably ontogenetic stage (Schwarz et al. 2007). *Plateosaurus* further appears to resemble *Europasaurus* in that pneumatic features of adults are largely present in the late stage juvenile (MOS 3 sensu Carballido and Sander 2014), however the earlier ontogenetic development in *Plateosaurus* remains unclear due to a lack of individuals pertaining to even earlier ontogenetic stages.

Conclusions

The discovery of a new, small-bodied (ca. 2.3 m total length, ca. 40–60 kg body mass) individual of *Plateosaurus* in the middle bone bed at Frick, Switzerland represents the first remains of a *Plateosaurus* significantly below 5 m total body length (Sander 1992; Hofmann and Sander 2014) and the first substantially complete skeleton of an unequivocally juvenile *Plateosaurus* (Fig. 14). The almost complete lack of suture fusion in the axial skeleton suggests the individual was an early-stage juvenile, which is corroborated by its small size. Caudal ribs and a probably referrable distal caudal vertebra furthermore provide some evidence for a progression of suture fusion in an anterior direction.

Comparison with the only previously described juvenile material of *Plateosaurus*, as well as adult skeletons of the genus, reveals a surprisingly similar postcranial morphology, despite the great size disparity. The axial skeleton in particular is almost identical to that of adults, displaying strongly developed patterns of laminae and fossae, which might have been important in guiding the development of air sacs during ontogeny.

Compared to adults, the juvenile skeleton has proportionately longer cervical vertebrae, similar to the condition observed in *Mussaurus*, but unlike that in *Massospondylus.* The appendicular skeleton differs from adults in some respects, such as the (possibly preservational) absence of a coracoid foramen and biceps tubercle, the concave proximal surface of the fifth metacarpal, and generally indistinct development of muscle scars. Within the forelimb, the manus is proportionately long, whereas the remaining elements are relatively short and gracile, providing no evidence for an adaptation towards quadrupedality, but further research on the presence of allometric growth in *Plateosaurus* is needed.

Most of the preserved osteology of juvenile *Plateosaurus* is consistent with that of adults, suggesting early development of morphologically adult characteristics in this taxon. This especially applies to the axial skeleton, that displays completely adult morphology except for the lack of suture fusion between most elements.

Acknowledgements

We would like to thank the entire team of the Sauriermuseum Frick and Saurierkommission Frick, especially Andrea Oettl and Ben Pabst (both MSF) for providing access to specimens and excavation site, invaluable information and advice and for preparation of the specimen. Tonwerke Keller AG provided access to the quarry for the purposes of excavation, which we are very grateful for. Georg Oleschinsky (Section Paleontology, Institute of Geoscience, University of Bonn, Germany) made suggestions that greatly improved the quality of specimen photographs. Nicole Klein and Xaver Donhauser (both Section Paleontology, Institute of Geoscience, University of Bonn) provided valuable discussions. We thank the Cantone of Aargau, Switzerland for continued funding of the excavation and preparation of the specimen. Blair McPhee (University of the Witwatersrand, Johannesburg, South Africa) and one anonymous reviewer made comments that greatly improved the quality of the manuscript.

References

Böhmer, C., Rauhut, O.W., and Wörheide, G. 2015. Correlation between Hox code and vertebral morphology in archosaurs. *Proceedings of Royal Society B* 282 (1810): 20150077.

Bonnan, M.F. 2007. Were the basal sauropodomorph dinosaurs *Plateosaurus* and *Massospondylus* habitual quadrupeds? *In*: P.M. Barrett and D.J. Batten (eds.), Evolution and Palaeobiology of Early Sauropodomorph Dinosaurs. *Special Papers in Palaeontology* 77: 139–155.

Brochu, C.A. 1996. Closure of neurocentral sutures during crocodilian ontogeny: implications for maturity assessment in fossil archosaurs. *Journal of Vertebrate Paleontology* 16: 49–62.

Butler, R.J., Barrett, P.M., and Gower, D.J. 2012. Reassessment of the evidence for postcranial skeletal pneumaticity in Triassic archosaurs, and the early evolution of the avian respiratory system. *PloS One* 7 (3): e34094.

Campione, N.E. 2016. *MASSTIMATE: Body Mass Estimation Equations for Vertebrates. R package version 1.3*. https://CRAN.R-project.org/package=MASSTIMATE

Campione, N.E., Evans, D.C., Brown, C.M., and Carrano, M.T. 2014. Body mass estimation in non-avian bipeds using a theoretical conversion to quadruped stylopodial proportions. *Methods in Ecology and Evolution* 5: 913–923.

Carballido, J.L. and Sander, P.M. 2014. Postcranial axial skeleton of *Europasaurus holgeri* (Dinosauria, Sauropoda) from the Upper Jurassic of Germany: implications for sauropod ontogeny and phylogenetic relationships of basal Macronaria. *Journal of Systematic Palaeontology* 12: 335–387.

Chapelle, K.E.J., Fernandez, V., and Choiniere, J.N. 2020. Conserved in-ovo cranial ossification sequences of extant saurians allow estimation of embryonic dinosaur developmental stages. *Scientific Reports* 10 (1): 4224.

Fechner, R. and Gößling, R. 2014. The gastralial apparatus of *Plateosaurus engelhardti*: morphological description and soft-tissue reconstruction. *Palaeontologia Electronica* 17 (1): 1–11.

Fraas, E. 1913. Die neuesten Dinosaurierfunde in der Schwäbischen Trias. *Naturwissenschaften* 1 (45): 1097–1100.

Galton, P.M. 1984. Cranial anatomy of the prosauropod dinosaur Plateosaurus from the Knollenmergel (Middle Keuper, Upper Triassic) of Germany. I. Two complete skulls from Trossingen/Württ. with comments on the diet. *Geologica et Palaeontologica* 18: 139–171.

Galton, P.M. 1985. Cranial anatomy of the prosauropod dinosaur *Plateosaurus* from the Knollenmergel (Middle Keuper, Upper Triassic) of Germany. II. All the cranial material and details of soft-part anatomy. *Geologica et Palaeontologica* 19: 119–159.

Galton, P.M. 1986. Prosauropod dinosaur *Plateosaurus* (= *Gresslyosaurus*) (Saurischia: Sauropodomorpha) from the Upper Triassic of Switzerland. *Geologica et Palaeontologica* 20: 167–183.

Galton, P.M. 2000. The prosauropod dinosaur *Plateosaurus* Meyer, 1837 (Saurischia: Sauropodomorpha). I. The syntypes of *P. engelhardti* Meyer, 1837 (Upper Triassic, Germany), with notes on other European prosauropods with "distally straight" femora. *Neues Jahrbuch für Geologie und Paläontologie-Abhandlungen* 216: 233–275.

Galton, P.M. 2001. The prosauropod dinosaur *Plateosaurus* Meyer, 1837 (Saurischia: Sauropodomorpha; Upper Triassic). II. Notes on the referred species. *Revue de Paléobiologie* 20: 435–502.

Galton, P.M. 2012. Case 3560 *Plateosaurus engelhardti* Meyer, 1837 (Dinosauria, Sauropodomorpha): proposed replacement of unidentifiable name-bearing type by a neotype. *The Bulletin of Zoological Nomenclature* 69: 203–212.

Galton, P.M. 2013. Comment on *Plateosaurus* Meyer, 1837 (Dinosauria, Sauropodomorpha): proposed replacement of unidentifiable name-bearing type by a neotype (Case 3560; see BZN 69: 203–212, 295–296; 70: 120–121). *Bulletin of Zoological Nomenclature* 70: 205–206.

Galton, P.M. and Kermack, D. 2010. The anatomy of *Pantydraco caducus*, a very basal sauropodomorph dinosaur from the Rhaetian (Upper Triassic) of South Wales, UK. *Revue de Paléobiologie* 29: 341–404.

Galton, P.M. and Upchurch, P. 2004. Prosauropoda. *In*: D.B. Weishampel, P. Dodson, and H. Osmólska (eds.), *The Dinosauria*, 232–258. University of California Press, Berkely.

Gunga, H.-C., Suthau, T., Bellmann, A., Friedrich, A., Schwanebeck, T., Stoinski, S., Trippel, T., Kirsch, K., and Hellwich, O. 2007. Body mass estimations for *Plateosaurus engelhardti* using laser scanning and 3D reconstruction methods. *Naturwissenschaften* 94: 623–630.

Hofmann, R. and Sander, P.M. 2014. The first juvenile specimens of *Plateosaurus engelhardti* from Frick, Switzerland: isolated neural arches and their implications for developmental plasticity in a basal sauropodomorph. *PeerJ* 2: e458.

von Huene, F.R. 1907–1908. Die Dinosaurier der europäischen Triasformation mit Berücksichtigung der aussereuropäischen Vorkommnisse. *Geologische und Paläontologische Abhandlungen,* Supplement 1: 1–419.

von Huene, F.R.F. 1926. Vollständige Osteologie eines Plateosauriden aus dem Schwäbischen Keuper. *Geologische und Paläontologische Abhandlungen* 15 (2): 1–43.

von Huene, F.R.F. 1928. Lebensbild des Saurischier-Vorkommens im obersten Keuper von Trossingen in Württemberg. *Palaeobiologica* 1: 103–116.

von Huene, F.R.F. 1932. Die fossile Reptilordnung Saurischia: ihre Entwicklung und Geschichte. *Monographien zur Geologie und Paläontologie* 1 (4): 1–361.

Hugi, J. and Scheyer, T.M. 2012. Ossification sequences and associated ontogenetic changes in the bone histology of pachypleurosaurids from Monte San Giorgio (Switzerland/Italy). *Journal of Vertebrate Paleontology* 32: 315–327.

ICZN 2019. Opinion 2435 (Case 3560) *Plateosaurus* Meyer, 1837 (Dinosauria, Sauropodomorpha): new type species designated. *Bulletin of Zoological Nomenclature* 76: 144–145.

Jaekel, O. 1914. Über die Wirbeltierfunde in der Oberen Trias von Halberstadt. *Paläontologische Zeitschrift* 1: 155–215.

Janensch, W. 1947. Pneumatizität bei Wirbeln von Sauropoden und anderen Saurischiern. *Palaeontographica-Supplementbände* 7: 1–25.

Jordan, P., Pietsch, J.S., Bläsi, H., Furrer, H., Kündig, N., Looser, N., Wetzel, A., and Deplazes, G. 2016. The Middle to Late Triassic Bänkerjoch and Klettgau formations of northern Switzerland. *Swiss Journal of Geosciences* 109: 257–284.

Klein, N. and Sander, P.M. 2007. Bone histology and growth of the prosauropod dinosaur *Plateosaurus engelhardti* von Meyer, 1837 from the Norian Bonebeds of Trossingen (Germany) and Frick (Switzerland). *In*: P.M. Barrett and D.J. Batten (eds.), *Evolution and Palaeobiology of Early Sauropodomorph Dinosaurs, Special Papers in Palaeontology, Vol. 77*, 169–206. Wiley, Hoboken.

Lambertz, M., Bertozzo, F., and Sander, P.M. 2018. Bone histological correlates for air sacs and their implications for understanding the origin of the dinosaurian respiratory system. *Biology Letters* 14 (1): 20170514.

Langer, M.C., Franca, M.A., and Gabriel, S. 2007. The pectoral girdle and forelimb anatomy of the stem-sauropodomorph *Saturnalia tupiniquim* (Upper Triassic, Brazil). *In*: P.M. Barrett and D.J. Batten (eds.), Evolution and Palaeobiology of Early Sauropodomorph Dinosaurs. *Special Papers in Palaeontology* 77: 113–137.

Langer, M.C., McPhee, B.W., de Almeida Marsola, J.C., Roberto-da-Silva, L., and Cabreira, S.F. 2019. Anatomy of the dinosaur *Pampadromaeus* barberenai (Saurischia—Sauropodomorpha) from the Late Triassic Santa Maria Formation of southern Brazil. *PloS One* 14 (2): e0212543.

Mallison, H. 2010a. The digital *Plateosaurus* I: body mass, mass distribution, and posture assessed using CAD and CAE on a digitally mounted complete skeleton. *Palaeontologia Electronica* 13 (13.2).

Mallison, H. 2010b. The digital *Plateosaurus* II: an assessment of the range of motion of the limbs and vertebral column and of previous reconstructions using a digital skeletal mount. *Acta Palaeontologica Polonica* 55: 433–458.

Marsh, O.C. 1895. ART. LV. On the affinities and classification of the dinosaurian reptiles. *American Journal of Science (1880–1910)* 50 (300): 483.

Melstrom, K.M., D'Emic, M.D., Chure, D., and Wilson, J.A. 2016. A juvenile sauropod dinosaur from the Late Jurassic of Utah, U.S.A., presents further evidence of an avian style air-sac system. *Journal of Vertebrate Paleontology* 36 (4): e1111898.

von Meyer, H. 1837. Mittheilungen, an Professor Bronn gerichtet. *Neues Jahrbuch für Geologie und Paläontologie* 1837: 314–316.

Moser, M. 2003. *Plateosaurus engelhardti* Meyer, 1837 (Dinosauria: Sauropodomorpha) aus dem Feuerletten (Mittelkeuper; Obertrias) von Bayern. *Zitteliana* 24: 3–186.

Myhrvold, N.P. 2013. Revisiting the estimation of dinosaur growth rates. *PloS one* 8 (12): e81917.

Otero, A., Cuff, A.R., Allen, V., Sumner-Rooney, L., Pol, D., and Hutchinson, J.R. 2019. Ontogenetic changes in the body plan of the sauropodomorph dinosaur *Mussaurus patagonicus* reveal shifts of locomotor stance during growth. *Scientific Reports* 9 (1): 7614.

Owen, R.1841. Report on British fossil reptiles, Part II. *Report for the British Association for the Advancement of Science* 1841: 60–294.

Prieto-Márquez, A. and Norell, M.A. 2011. Redescription of a nearly complete skull of *Plateosaurus* (Dinosauria: Sauropodomorpha) from the Late Triassic of Trossingen (Germany). *American Museum Novitates* 3727: 1–58.

R Core Team 2018. *R: A Language and Environment for Statistical Computing.* R Foundation for Statistical Computing, Vienna. https://www.R-project.org/

Rauhut, O.W.M., Holwerda, F.M., and Furrer, H. 2020. A derived sauropodiform dinosaur and other sauropodomorph material from the Late Triassic of Canton Schaffhausen, Switzerland. *Swiss Journal of Geosciences* 113: 8.

Reiss, S. and Mallison, H. 2014. Motion range of the manus of *Plateosaurus engelhardti* von Meyer, 1837. *Palaeontologia Electronica* 17 (1): 1–19.

Reisz, R.R., Evans, D.C., Sues, H.-D., and Scott, D. 2010. Embryonic skeletal anatomy of the sauropodomorph dinosaur *Massospondylus* from the Lower Jurassic of South Africa. *Journal of Vertebrate Paleontology* 30: 1653–1665.

Reisz, R.R., Evans, D.C., Roberts, E.M., Sues, H.-D., and Yates, A.M. 2012. Oldest known dinosaurian nesting site and reproductive biology of the Early Jurassic sauropodomorph *Massospondylus*. *Proceedings of the National Academy of Sciences* 109: 2428–2433.

Reisz, R.R., Scott, D., Sues, H.-D., Evans, D.C., and Raath, M.A. 2005. Embryos of an Early Jurassic prosauropod dinosaur and their evolutionary significance. *Science* 309: 761–764.

Remes, K. 2008. *Evolution of the Pectoral Girdle and Forelimb in Sauropodomorpha (Dinosauria, Saurischia): Osteology, Myology and Function*. 355 pp. Dissertation, Ludwig-Maximilians-Universität, Munich.

Romer, A.S. 1976. *Osteology of the Reptiles. 3rd Edition*. 772 pp. University of Chicago Press, Chicago.

Sander, P.M. 1992. The Norian *Plateosaurus* bonebeds of central Europe and their taphonomy. *Palaeogeography, Palaeoclimatology, Palaeoecology* 93: 255–299.

Sander, P.M. and Klein, N. 2005. Developmental plasticity in the life history of a prosauropod dinosaur. *Science* 310: 1800–1802.

Schwarz, D., Ikejiri, T., Breithaupt, B.H., Sander, P.M., and Klein, N. 2007. A nearly complete skeleton of an early juvenile diplodocid (Dinosauria: Sauropoda) from the Lower Morrison Formation (Late Jurassic) of north central Wyoming and its implications for early ontogeny and pneumaticity in sauropods. *Historical Biology* 19: 225–253.

Sues, H.-D. 2013. Comment on Case 3560: *Plateosaurus engelhardti* Meyer, 1837 (Dinosauria, Sauropodomorpha): proposed replacement of unidentifiable name-bearing type by a neotype (Case 3560). *Bulletin of Zoological Nomenclature* 70: 120–121.

Van Heerden, J. 1997. Prosauropods. *In*: J.O. Farlow and M.K. Brett-Surman (eds.), *The Complete Dinosaur*, 242–263. Indiana University Press, Bloomington.

Wedel, M.J. 2006. Origin of postcranial skeletal pneumaticity in dinosaurs. *Integrative Zoology* 1: 80–85.

Wedel, M.J. 2007. What pneumaticity tells us about "prosauropods", and vice versa. *In*: P.M. Barrett and D.J. Batten (eds.), Evolution and Palaeobiology of Early Sauropodomorph Dinosaurs. *Special Papers in Palaeontology* 77: 207–222.

Wedel, M.J. 2009. Evidence for bird-like air sacs in saurischian dinosaurs. *Journal of Experimental Zoology Part A: Ecological Genetics and Physiology* 311: 611–628.

Weishampel, D.B. and Chapman, R.E. 1990. Morphometric study of *Plateosaurus* from Trossingen (Baden-Württemberg, Federal Republic of Germany). *In*: K. Carpenter and P.J. Currie (eds.), *Dinosaur Systematics: Approaches and Perspectives*, 43–51. Cambridge University Press, Cambridge.

Wilson, J.A. 1999. A nomenclature for vertebral laminae in sauropods and other saurischian dinosaurs. *Journal of Vertebrate Paleontology* 19: 639–653.

Wilson, J.A., D'Emic, M.D., Ikejiri, T., Moacdieh, E.M., and Whitlock, J.A. 2011. A nomenclature for vertebral fossae in sauropods and other saurischian dinosaurs. *PLoS One* 6 (2): e17114.

Yates, A.M. 2003. The species taxonomy of the sauropodomorph dinosaurs from the Löwenstein Formation (Norian, Late Triassic) of Germany. *Palaeontology* 46: 317–337.

Yates, A.M., Bonnan, M.F., Neveling, J., Chinsamy, A., and Blackbeard, M.G. 2010. A new transitional sauropodomorph dinosaur from the Early Jurassic of South Africa and the evolution of sauropod feeding and quadrupedalism. *Proceedings of the Royal Society of London B: Biological Sciences* 277: 787–794.

Yates, A.M., Wedel, M.J., and Bonnan, M.F. 2012. The early evolution of postcranial skeletal pneumaticity in sauropodomorph dinosaurs. *Acta Palaeontologica Polonica* 57: 85–100.

Zahner, M. and Brinkmann, W. 2019. A Triassic averostran-line theropod from Switzerland and the early evolution of dinosaurs. *Nature Ecology & Evolution* 3 (8): 1146–1152.